

Spallative-cavitative ablation
is a main mechanism of removal of matter
by ultrashort laser pulse in case of any substances
(metals, semiconductors, dielectrics)
and any light wavelength

- ▣ N.A.Inogamov, V.V.Zhakhovskii, V.A.Khokhlov, V.V.Shepelev,
- ▣ Yu.V.Petrov, S.I.Anisimov, M.B.Agranat, S.I.Ashitkov, P.S.Komarov,
- ▣ A.V.Ovchinnikov, D.S.Sitnikov, V.E.Fortov, A.Ya.Faenov, I.Y.Skobelev,
T.A. Pikuz

- ▣ * L.D. Landau Institute for Theoretical Physics, RAS
- ▣ * Joint Institute for High Temperatures, RAS
- ▣ * University of South Florida, Tampa, USA
- ▣ * Kansai Photon Science Institute, Japan Atomic Energy Agency, Kyoto,
Japan
- ▣ * Institute for Computer Aided Design, RAS
- ▣ * The Graduate School for the Creation of New Photonics Industries,
Shizuoka, Japan

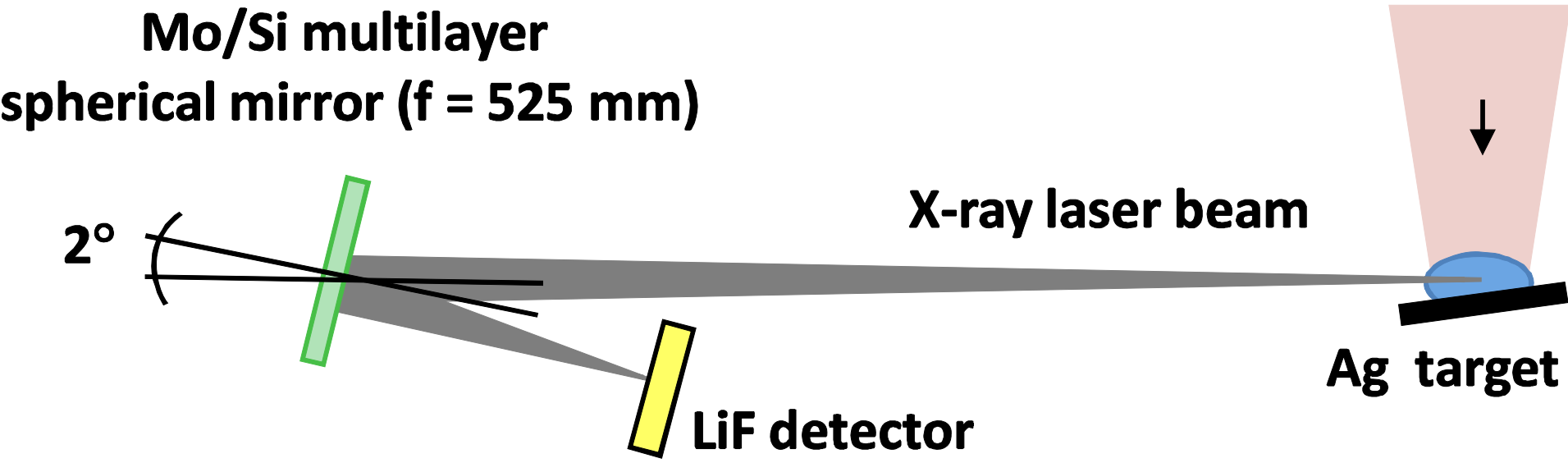
Motivation

□ Toolbox:

- Ultrashort IR, **viz.** lasers $h\nu \sim 1\text{eV}$, pulse duration τ_L from few cycles
- Fs-ps XUV - **X-ray** lasers $h\nu \sim 0.1\text{-}10\text{ keV}$:
- 1) Transient-collisional scheme
- 2) High order harmonic generation by fs IR, viz. laser
- 3) X-ray free electron laser, XFEL

□ Applications:

- Surface micromachining, Nano-particle synthesis, Mass-spectrometry, etc



Motivation

□ Toolbox:

- Ultrashort IR, viz. lasers $h\nu \sim 1\text{eV}$, pulse duration τ_L from few cycles
- Fs-ps XUV – X-ray lasers $h\nu \sim 0.1\text{-}10\text{ keV}$:
- 1) Transient-collisional scheme
- 2) High order harmonic generation by fs IR, viz. laser
- 3) X-ray free electron laser, XFEL

□ Applications:

- Surface micromachining, Nano-particle synthesis, Mass-spectrometry, etc

□ Fundamental Problems:

- **(1)** Electron-ion non-equilibrium states with highly excited electron subsystem, two-temperature warm dense matter(2T WDM)
- **(2)** Metastable decay, foaming, nanostructuring

Physical processes

- Two-temperature WDM

- Absorption: $h\nu \rightarrow$ electrons (IR, viz. v. X-ray)

- Electron-electron relaxation

- Electron-ion relaxation

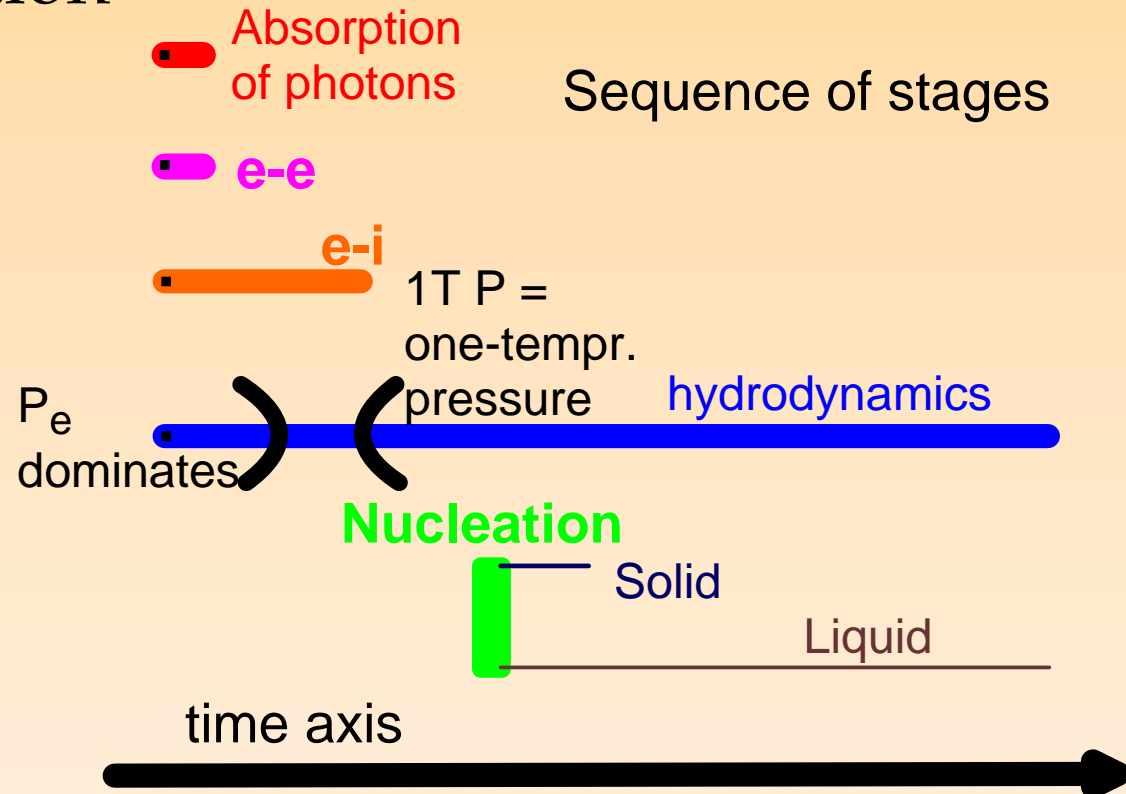
- Metastable decay

- Hydrodynamics:

- Expansion,

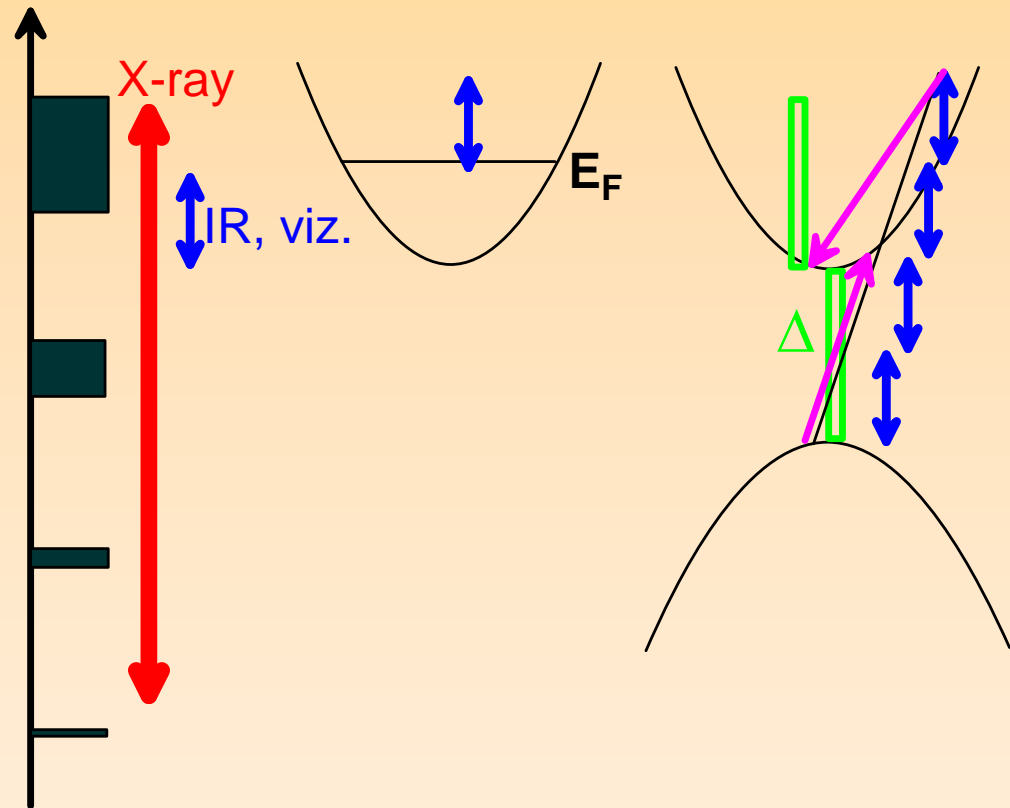
- Transition to metastable state,

- Nucleation (in solid state v. in liquid state)



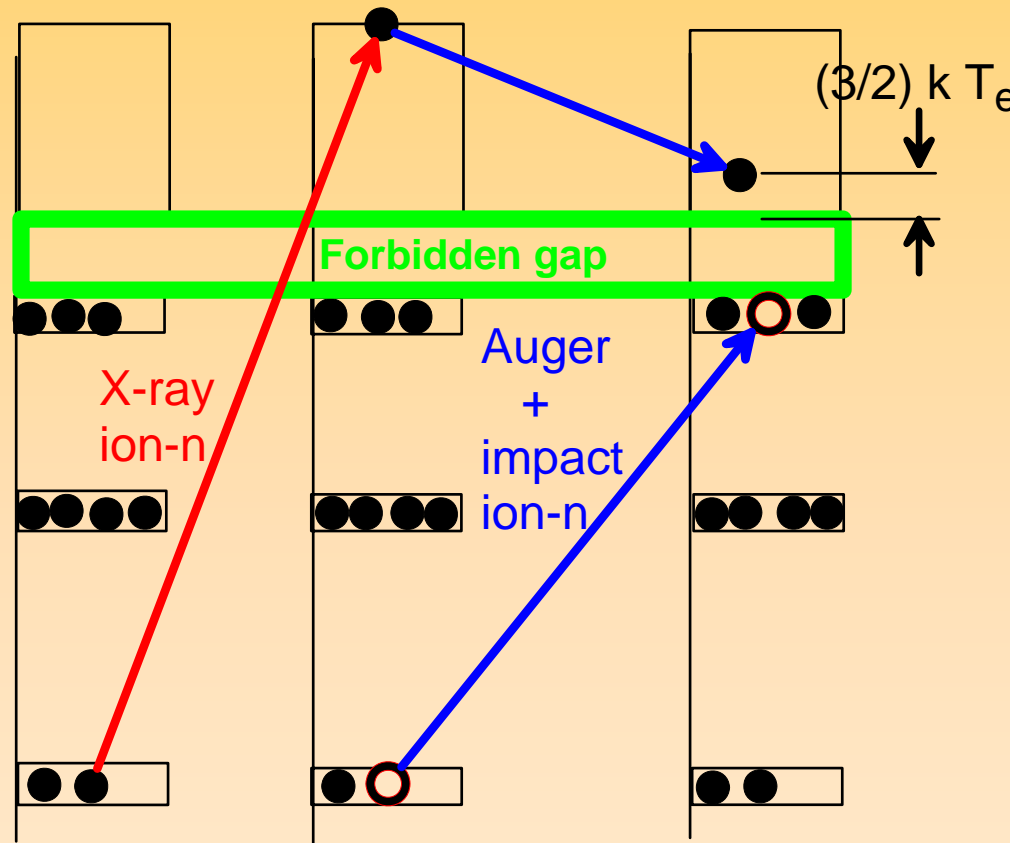
Optical absorption

- IR, viz. versus XUV-X-ray
- IR, viz. lasers have photons with energies $h\nu \sim$ energy of the valence bands, while the X-ray quanta ionizes the internal shells
- Metals
- Semiconductors and dielectrics :
- Multi-photon ion-n
- Tunnel ionization
- Keldysh expression
- Electron impact ionization and avalanche



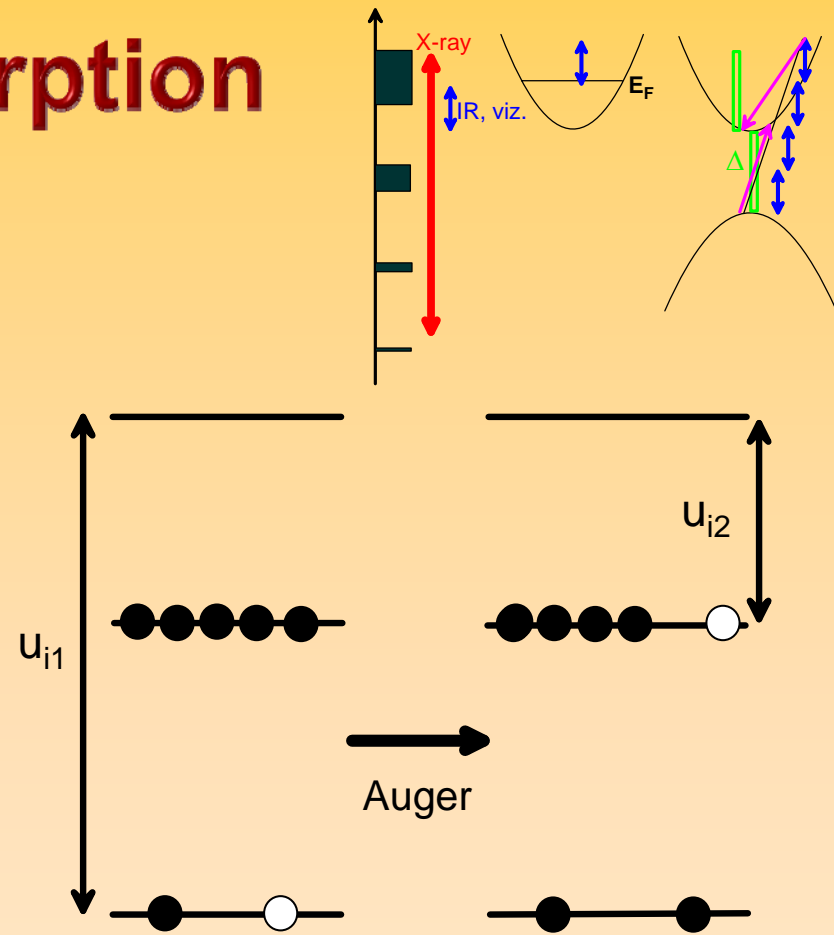
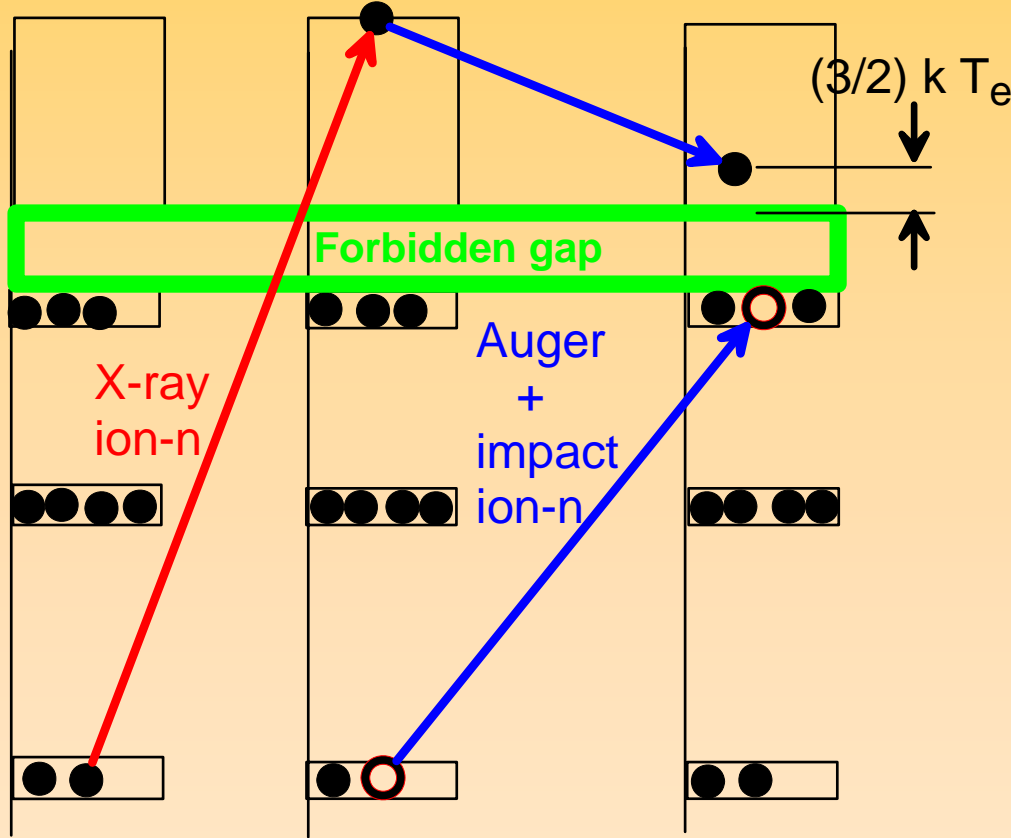
X-ray absorption

- X-ray photons knock out electrons from the deep levels making holes in the internal shells
- Appearance of deep holes triggers the Auger processes
- While appearance of energetic electrons starts impact ionization



□ This picture is drawn for substances with the gap. Similar scheme is applicable to metals. In metals energetic electrons finally transfer their energy to conductivity electrons

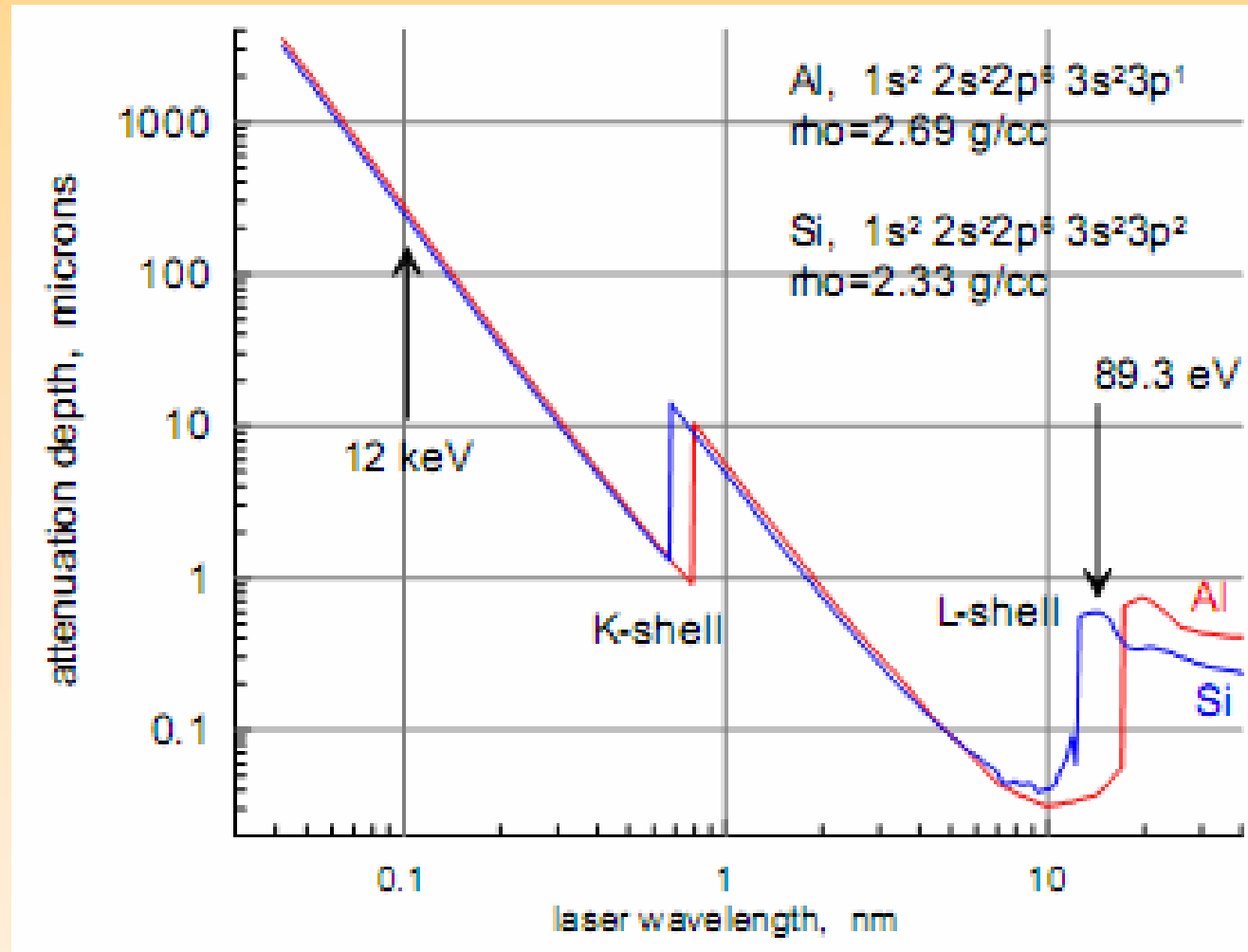
X-ray absorption



(1) Impact ionization starts immediately with the pulse = we have not wait when ionized electrons accumulate enough energy by inverse Bremsstrahlung to overcome the gap (no significant inverse Bremsstrahlung absorption), (2) no avalanche, (3) energy conservation

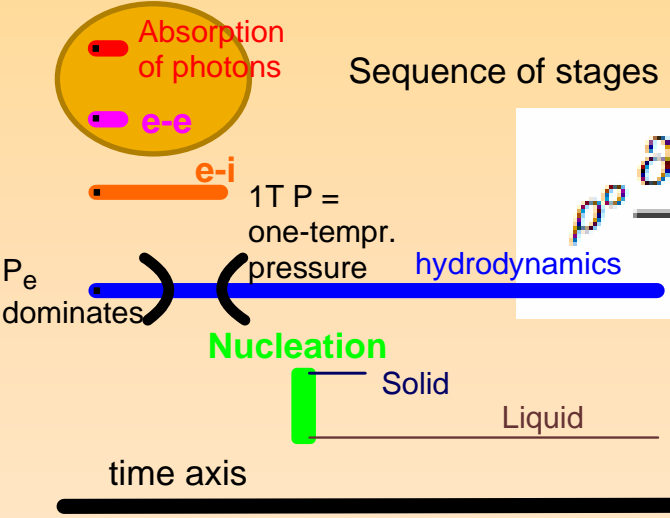
Attenuation depth

- Attenuation depth varies in a wide range with $h\nu$.
- Photon energy of the Ag X-ray laser is between the L-edges for Al and Si. Therefore the attenuation depths for Al (37 nm) and Si (590 nm) are very different.
- Taken from Henke



Equations

□ We exclude short stage when electrons are non-Maxwellian. The equations are written for electron and ion subsystems which may be described by average concentration of free electrons and two temperatures T_e and T_i .



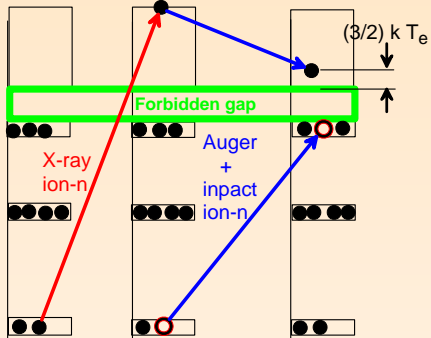
□ Energy conservation!

$$\rho^o \frac{\partial E_e^{sum} / \rho}{\partial t} = - \frac{\partial q_e}{\partial x^o} - p_e \frac{\partial u}{\partial x^o} - \frac{\rho^o}{\rho} \dot{E}_{ei} + \frac{\rho^o}{\rho} Q,$$

Equations are written in Lagrangian coordinate x^o

$$E_e^{sum} = n_e u_{i2} + E_e \quad E_e = (3/2) k_B T_e$$

$$\frac{\partial n_e}{\partial t} = - \frac{\rho}{\rho^o} \frac{\partial j}{\partial x^o} - \frac{\rho}{\rho^o} n_e \frac{\partial u}{\partial x^o} + \frac{Q}{u_{i2}} + \nu_{imp} n_e - k_3 n_e^3 - \nu_{ph} n_e$$



$$\rho^o \frac{\partial E_i / \rho}{\partial t} = - \frac{\partial q_i}{\partial x^o} - p_i \frac{\partial u}{\partial x^o} + \frac{\rho^o}{\rho} \dot{E}_{ei},$$

Equations

- We have considered ablation of LiF dielectrics by X-ray laser with 89.3 eV photons and short pulse duration 7 ps
- Electron and phonon thermal conductivity and ambipolar diffusion may be neglected for our time interval <100 ps
- Potential energy of holes u_{i2} was taken $\sim \Delta$ - width of the gap
- Electron impact frequency ν_{imp} was taken from [Biberman, Vorobyev, Yakubov, 1987; Sobelman, Vainshtein, Yukov, 2007]
- $E_e^{sum} = n_e u_{i2} + E_e$. $\dot{E}_{ei} = A E_e$, $A \sim 3 \cdot 10^{11} \text{ s}^{-1}$
- The coefficient of three-body recombination k_3 was calculated from condition of detailed equilibrium

$$\rho^o \frac{\partial E_e^{sum} / \rho}{\partial t} = - \frac{\partial q_e}{\partial x^o} - p_e \frac{\partial u}{\partial x^o} - \frac{\rho^o}{\rho} \dot{E}_{ei} + \frac{\rho^o}{\rho} Q,$$

$$\frac{\partial n_e}{\partial t} = - \frac{\rho}{\rho^o} \frac{\partial j}{\partial x^o} - \frac{\rho}{\rho^o} n_e \frac{\partial u}{\partial x^o} + \frac{Q}{u_{i2}} + \nu_{imp} n_e - k_3 n_e^3 - \nu_{ph} n_e$$

Equations averaged at the attenuation depth

- For dielectrics thermal conduction and diffusion are small – we can neglect them at our time scale. The averaged equations are

$$dn_e/dt = Q/u_{i2} + \nu_{imp}n_e - \kappa_{rec}n_e^3, \quad Q = (F/(\sqrt{\pi}d_T\tau)) \exp(-t^2/\tau^2),$$

$$dE_e^s/dt = Q - \dot{E}_{ea}, \quad E_e^s = n_e u_{i2} + E_e, \quad E_e = (3/2)n_e T_e,$$

$$CdT_{at}/dt = \dot{E}_{ea}, \quad C \approx 6k_B n_c, \quad n_c \approx 6 \cdot 10^{22} \text{ cm}^{-3}, \quad \dot{E}_{ea} = AE_e,$$

Increase and decrease of free electron population and electron temperature T_e

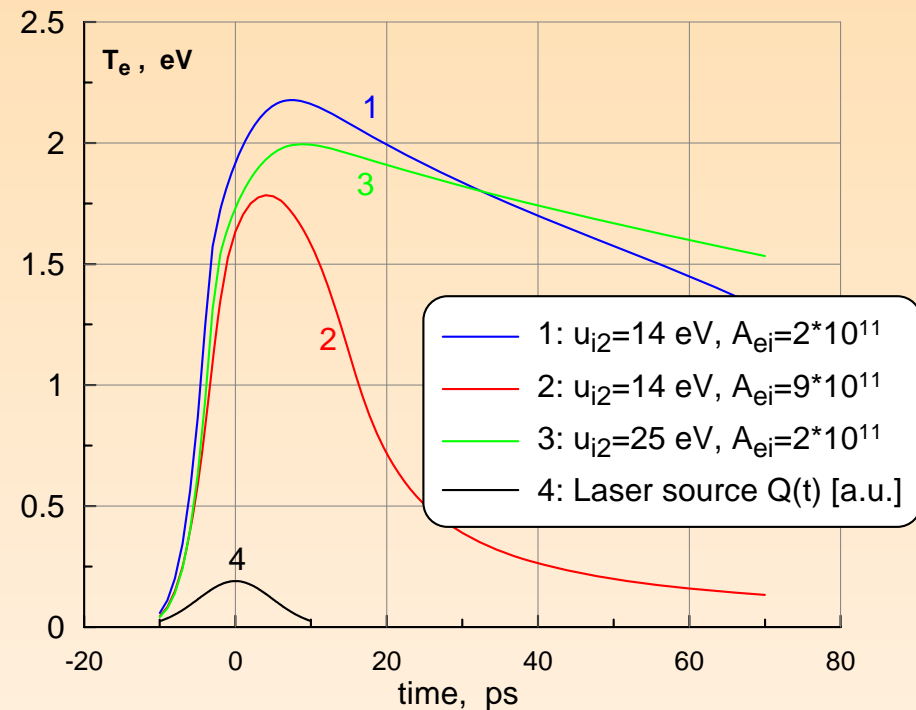
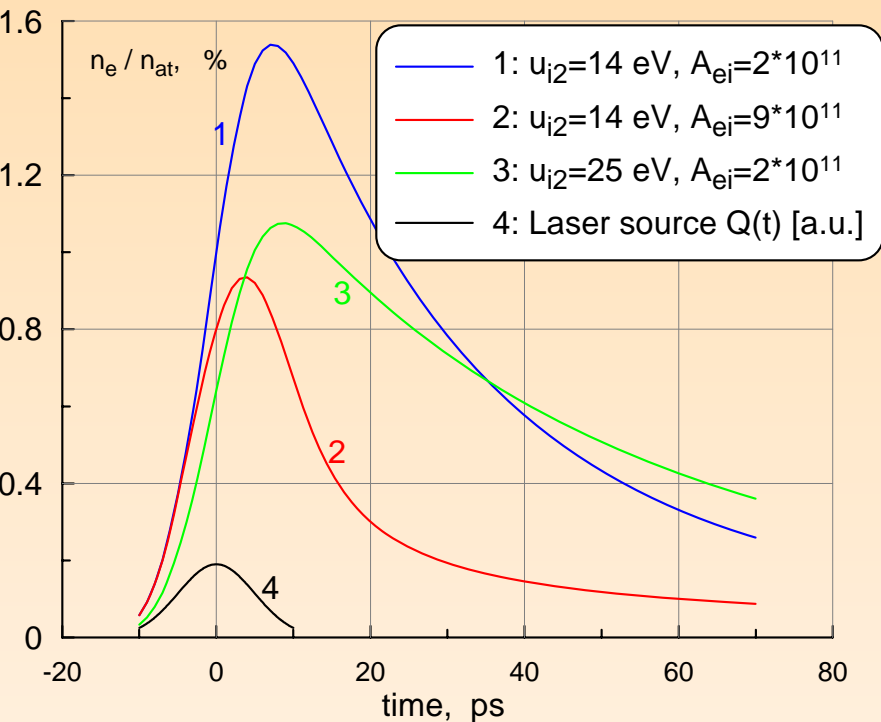
□ Pulse duration 7 ps, $F_{\text{abs}} = 10 \text{ mJ/cm}^2$, $h\nu = 89.3 \text{ eV}$

Att. depth LiF=28 nm

$$dn_e/dt = Q/u_{i2} + \nu_{\text{imp}}n_e - \kappa_{\text{rec}}n_e^3, \quad Q = (F/(\sqrt{\pi}d_T\tau)) \exp(-t^2/\tau^2),$$

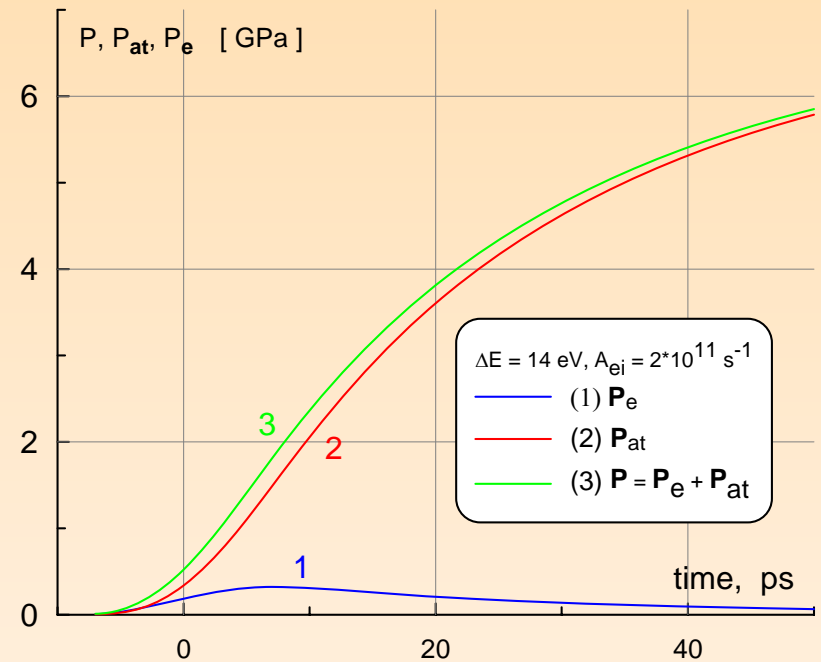
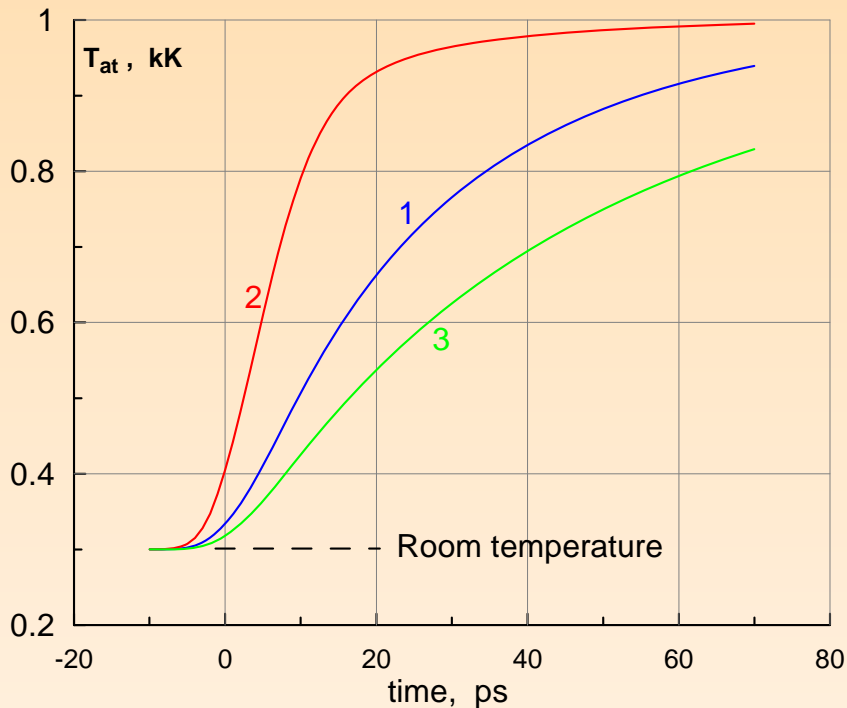
$$dE_e^s/dt = Q - \dot{E}_{ea}, \quad E_e^s = n_e u_{i2} + E_e, \quad E_e = (3/2)n_e T_e,$$

$$CdT_{at}/dt = \dot{E}_{ea}, \quad C \approx 6k_B n_c, \quad n_c \approx 6 \cdot 10^{22} \text{ cm}^{-3}, \quad \dot{E}_{ea} = AE_e,$$



Increase of temperature T_i and pressure by absorption of X-ray pulse

- Simulations show that temperature and pressure rise approximately follows X-ray laser pulse

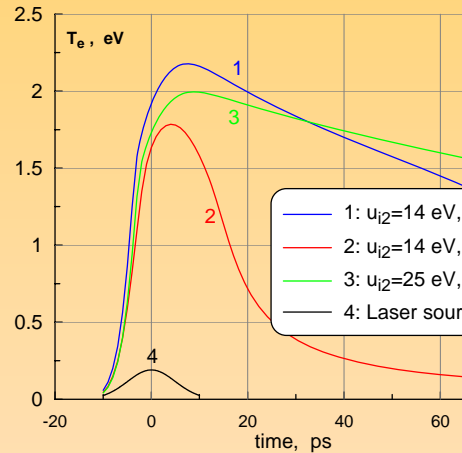


Generation of acoustic wave

$$\rho^o \frac{\partial E_e^{sum} / \rho}{\partial t} = - \frac{\partial q_e}{\partial x^o} - p_e \frac{\partial u}{\partial x^o} - \frac{\rho^o}{\rho} \dot{E}_{ei} + \frac{\rho^o}{\rho} Q,$$

$$\frac{\partial n_e}{\partial t} = - \frac{\rho}{\rho^o} \frac{\partial j}{\partial x^o} - \frac{\rho}{\rho^o} n_e \frac{\partial u}{\partial x^o} + \frac{Q}{u_{i2}} + \nu_{imp} n_e - k_3 n_e^3 - \nu_{ph} n_e$$

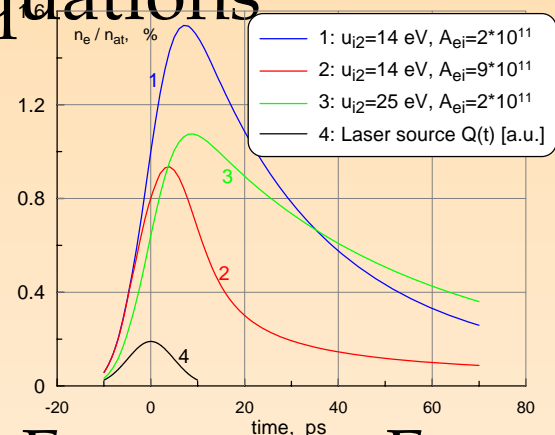
$$\rho^o \frac{\partial E_i / \rho}{\partial t} = - \frac{\partial q_i}{\partial x^o} - p_i \frac{\partial u}{\partial x^o} + \frac{\rho^o}{\rho} \dot{E}_{ei},$$



To describe spatial profiles we solve equations

$$\rho^o \frac{\partial}{\partial t} \frac{E_e}{\rho} = \frac{\rho^o}{\rho} Q - \frac{\rho^o}{\rho} \dot{E}_{ea} - p_e \frac{\partial u}{\partial x^o}$$

$$\rho^o \partial(E_{at}/\rho)/\partial t = (\rho^o/\rho) \dot{E}_{ea} - p_{at} \partial u / \partial x^o$$

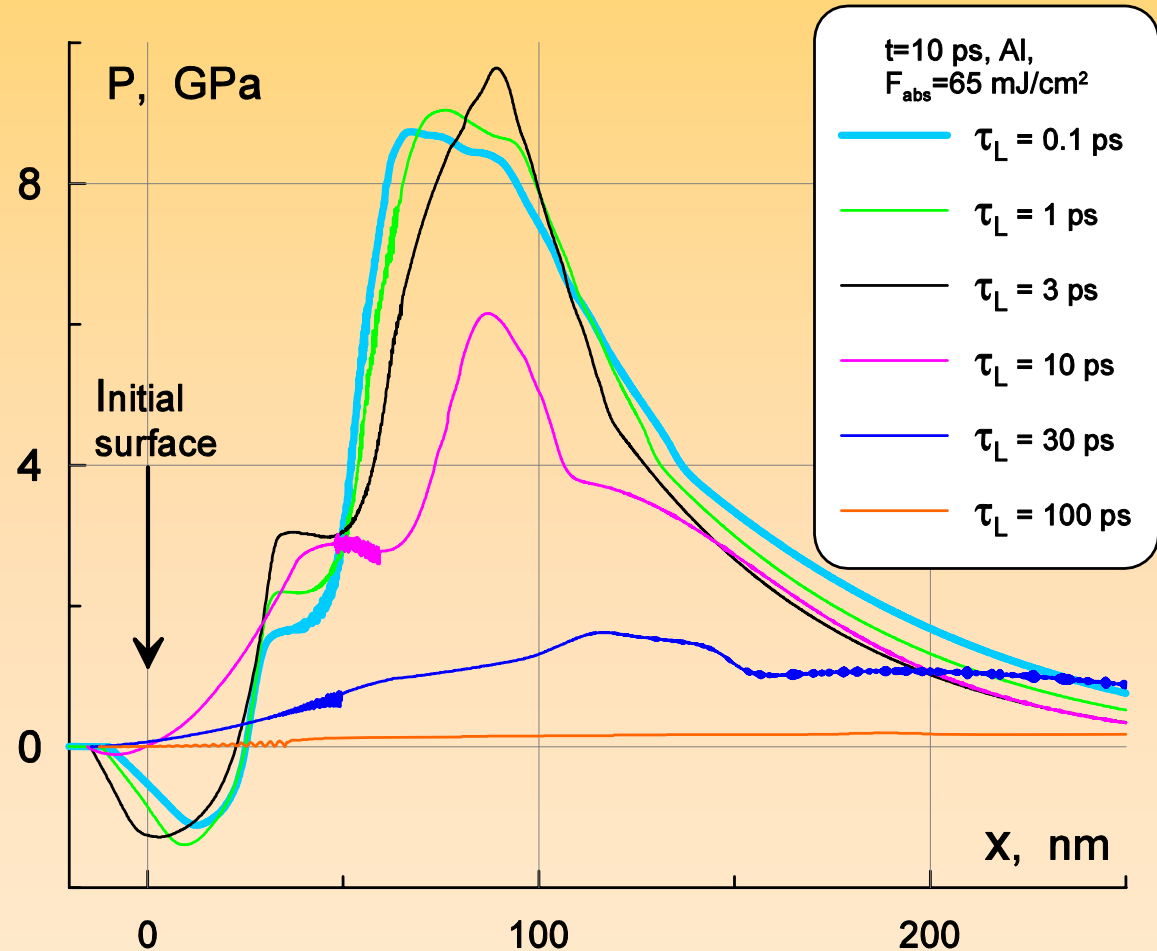


We neglect heat conductivity, write E_e except $E_e^{sum} = n_e u_{i2} + E_e$, and write e-i exchange \dot{E}_{ea} as

$A_1^*(T_e - T_i) = A_1^* T_e = A^* E_e$, as $E_e = (3/2) k T_e$, E_F is small

Short versus long pulses

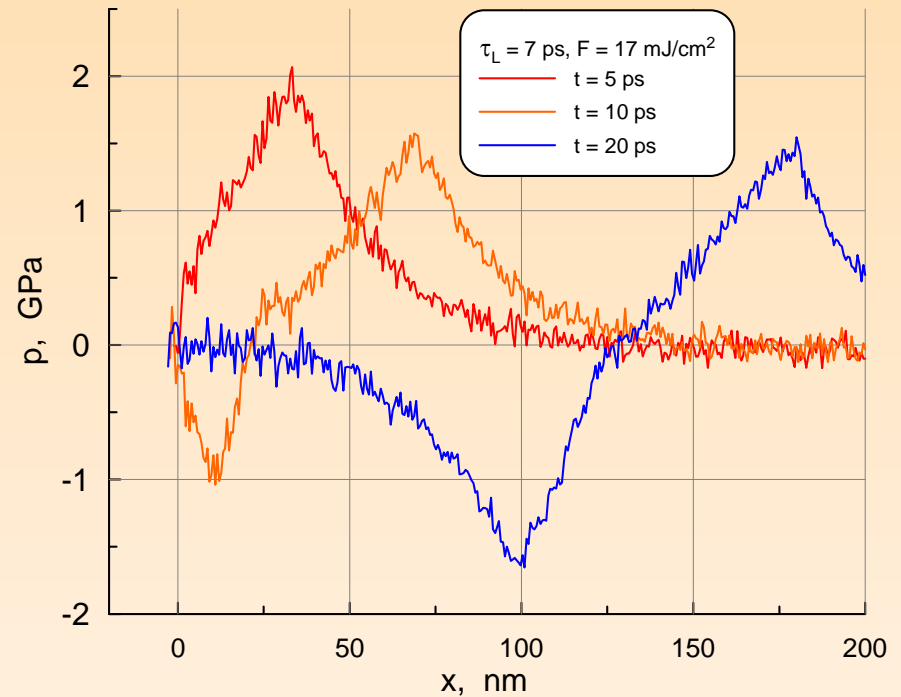
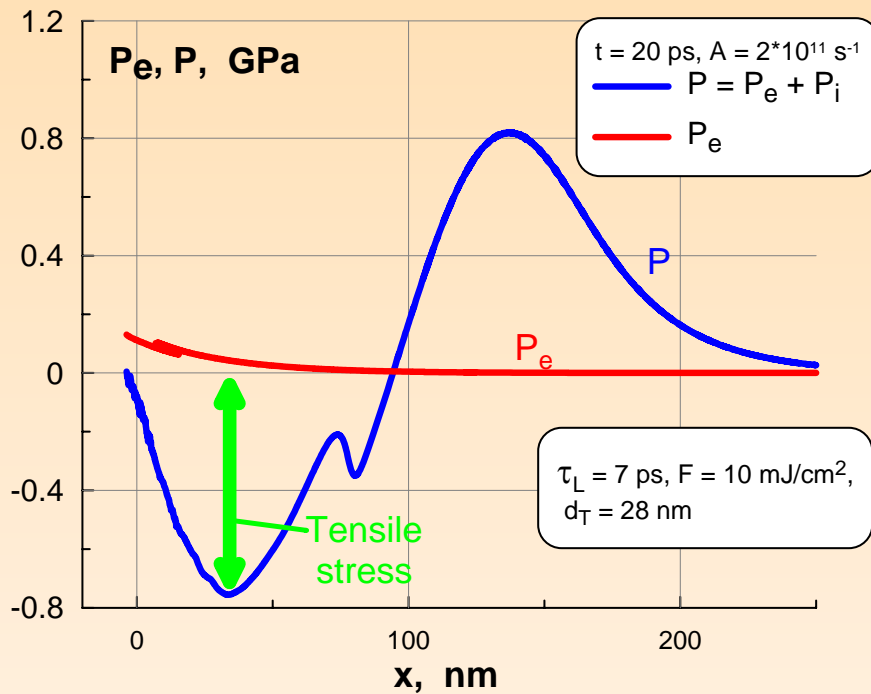
- To have significant mechanical effect the large pressures are necessary
- Maximum pressure is defined by energy absorbed during acoustic response time $t_s = d_T / c_s \sim 10$



Therefore short pulses are more effective in creation of high pressures

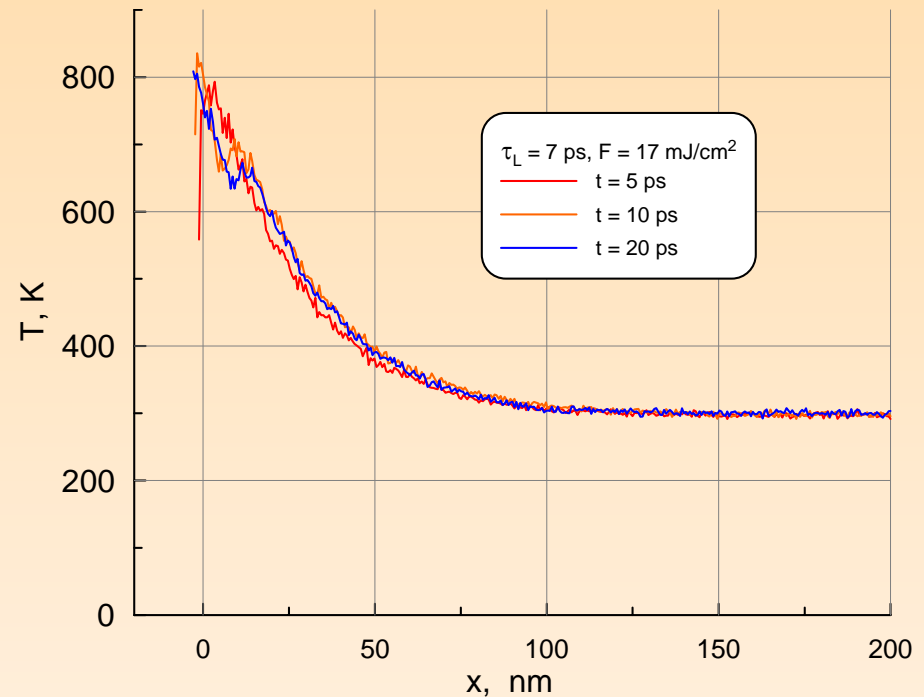
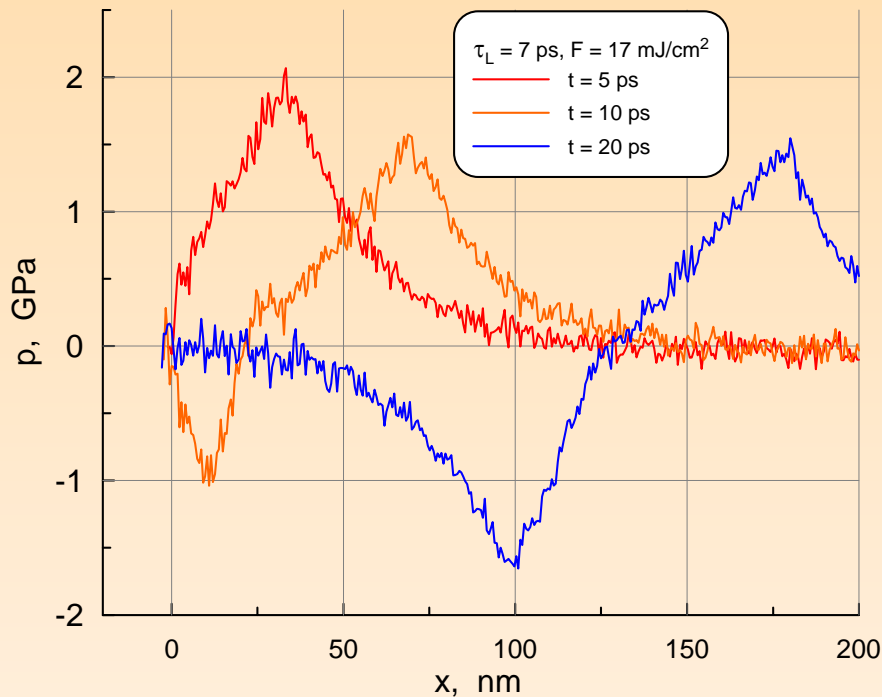
Short pulse X-ray laser creates tensile stress

- Examples with two-temperature hydrodynamic simulation and one-temperature molecular-dynamics (MD) simulation
- We have used power density \dot{E}_{ea} calculated by 2T code as input for MD simulation



Short pulse X-ray laser creates tensile stress

- Temperature field is “frozen” and does not change significantly at acoustic time scale when acoustic wave travels out from laser energy absorption layer



- Above we have considered:

- Absorption of X-ray photons

- Thermalization of electron subsystem

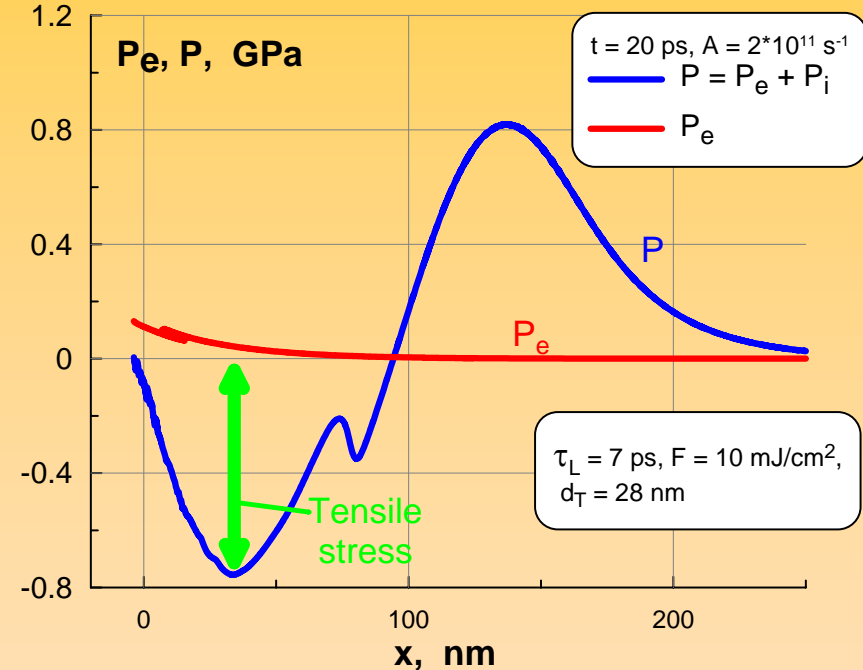
- Two-temperature equations describing electron-ion temperature relaxation and hydrodynamic motion

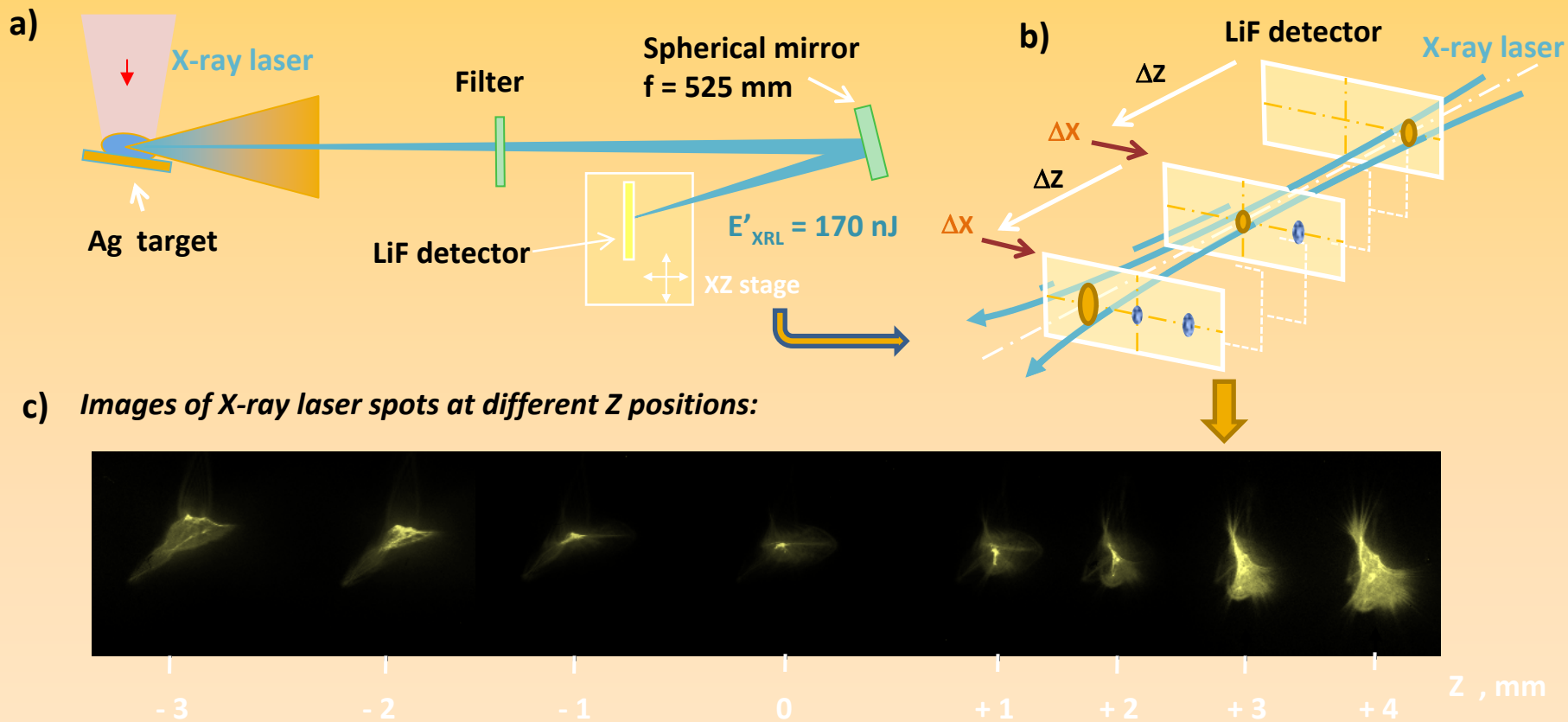
- Now we can conclude :

Short pulse X-ray laser creates tensile stress

- The amplitude of the tensile stress 8-10 kbar is enough to trigger the spallative ablation

- Material strength for PMMA = 8 kbar, Krasnyuk, Vovchenko et al., 2009





Experiments with spallative ablation by X-ray laser

Fig. 1

**AFM image of focal spot after irradiation
by full (10.2 mJ/cm²) XRL energy**

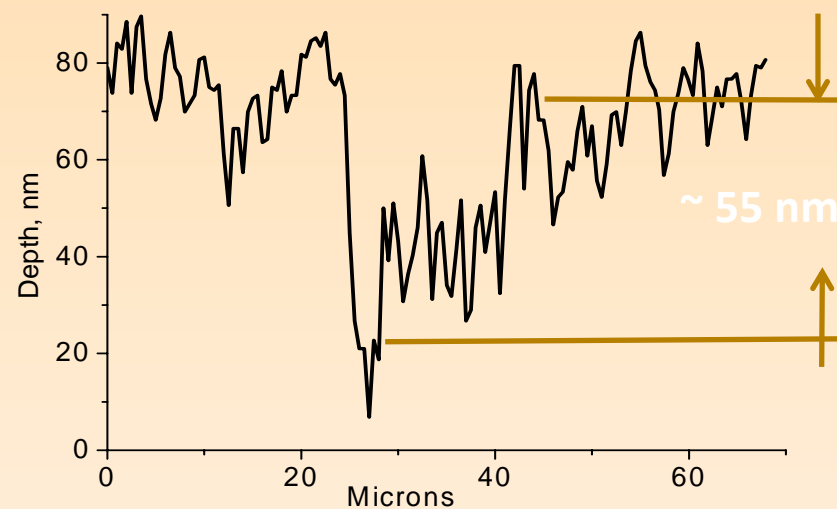
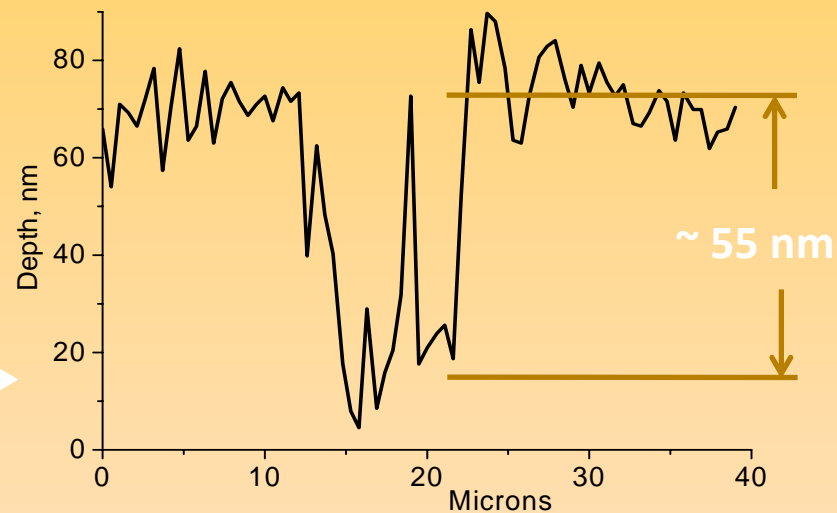
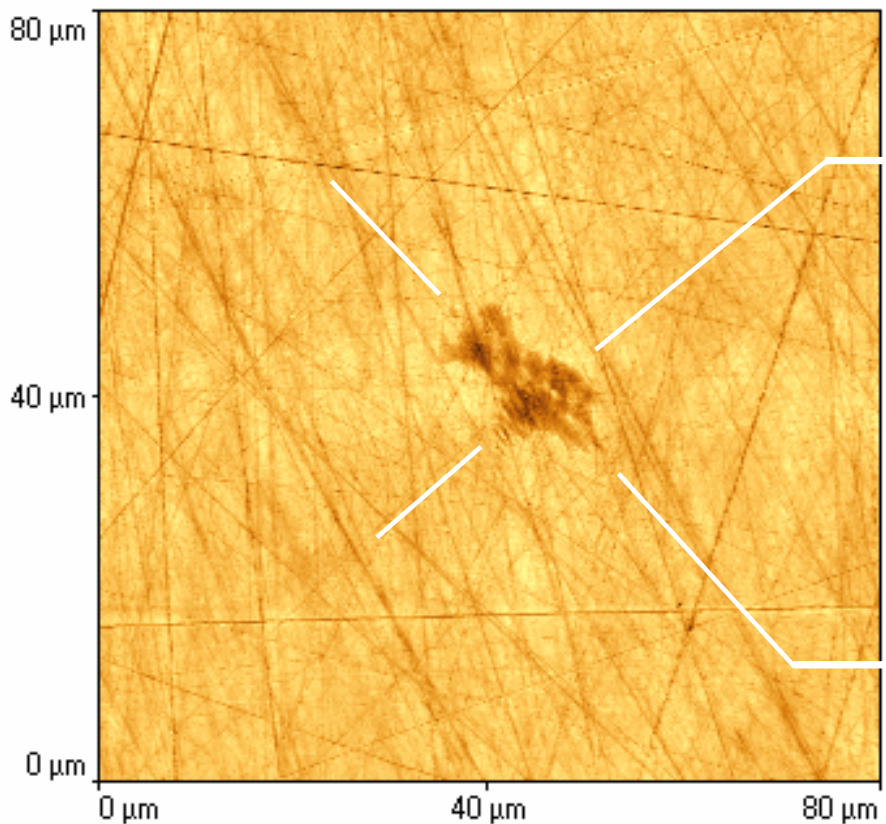
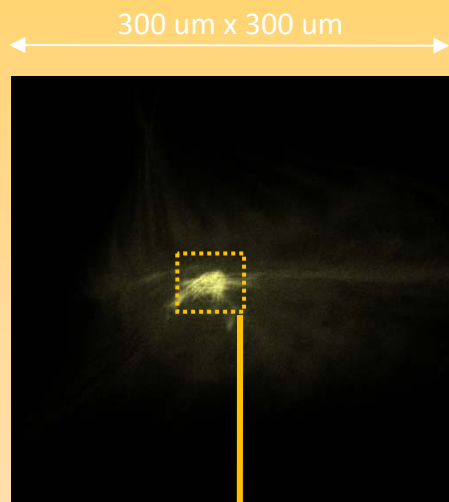


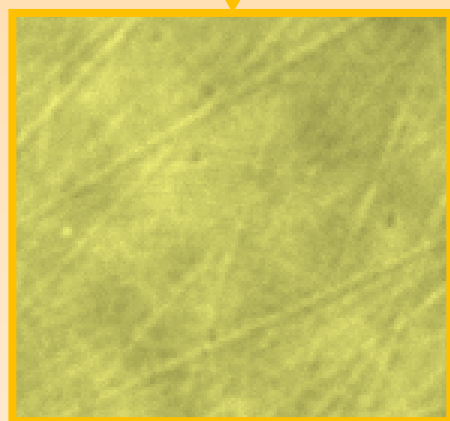
Fig. 2

1 laser shots $E = 5 \text{ mJ/cm}^2$, $8.5 \times 10^8 \text{ W/cm}^2$

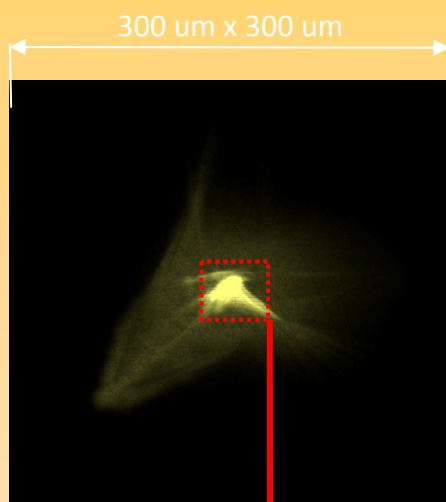
3 laser shots $E = 5 \text{ mJ/cm}^2$, $8.5 \times 10^8 \text{ W/cm}^2$



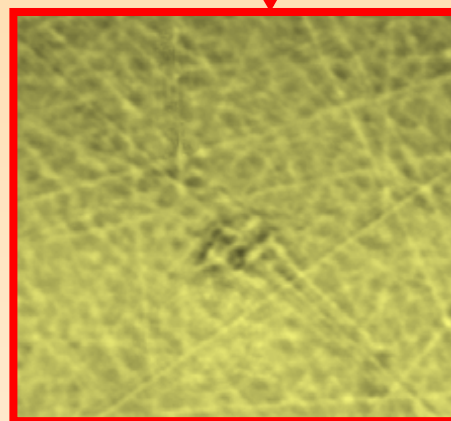
Luminescent image



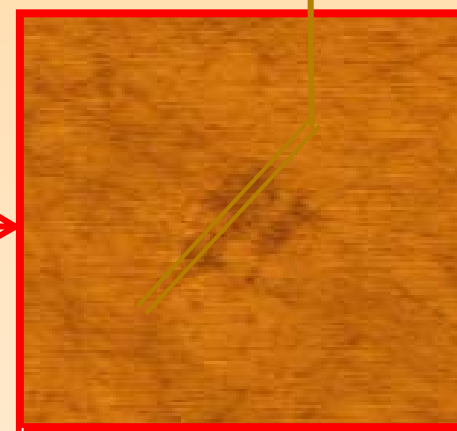
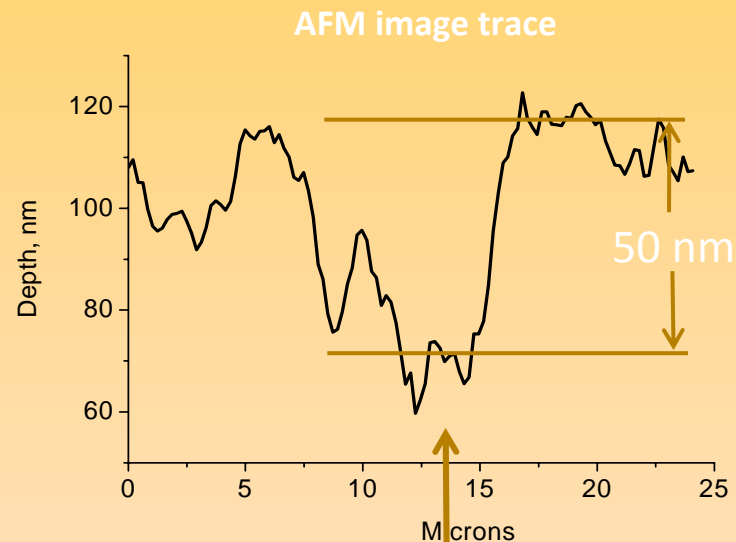
Visible image



Luminescent image



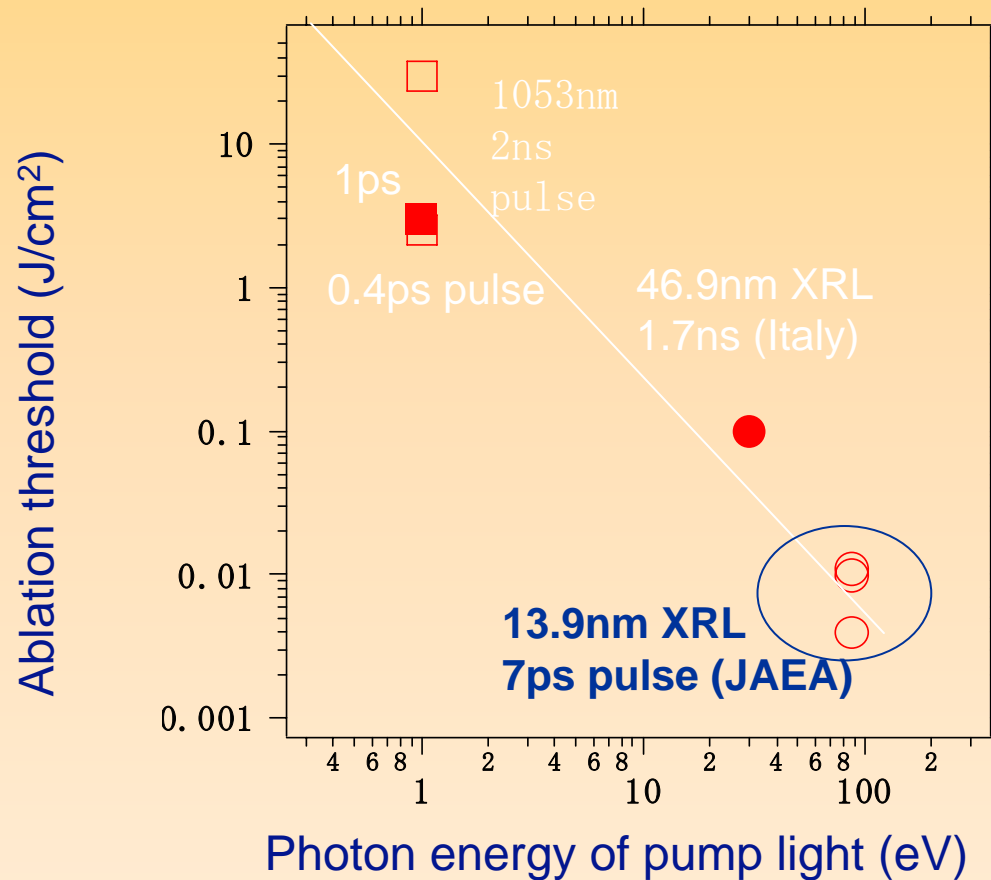
Visible image



AFM image

Fig. 3

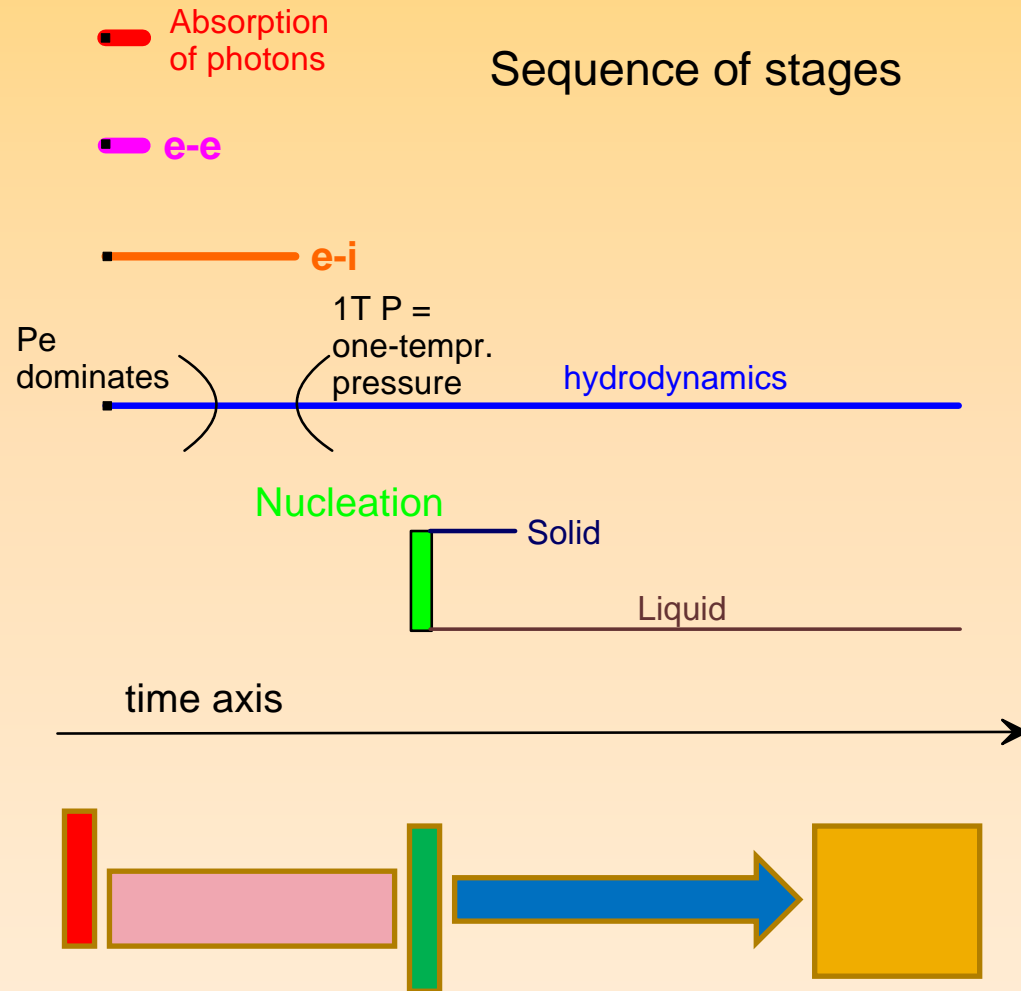
Pico-second XRL ablation shows drastic decrease of ablation threshold of energy fluency



Faenov, Inogamov, Zhakhovskii et al. Appl. Phys. Lett., 94, 231107 (2009)

“Contact interface” between laser initiation and development of the tensile field

- Short laser pulse creates stretching and tensile stress
- Laser may be optical, or –as was shown above– the X-ray laser
- $P < 0$ is the reason for nucleation-foaming-nanostructure formation
- For optical lasers this has been shown previously
- Now we extend this to the case of X-rays



Laser-acoustics-nucleation-foaming-nanostructuring : this is development in time

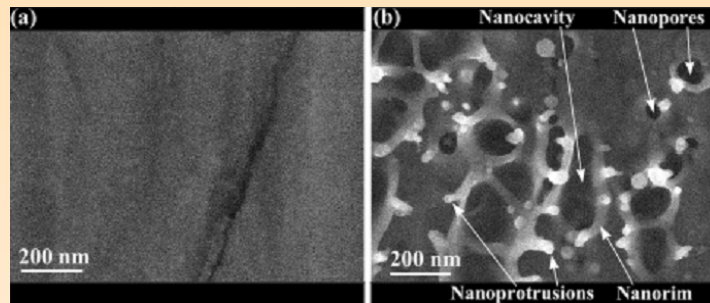
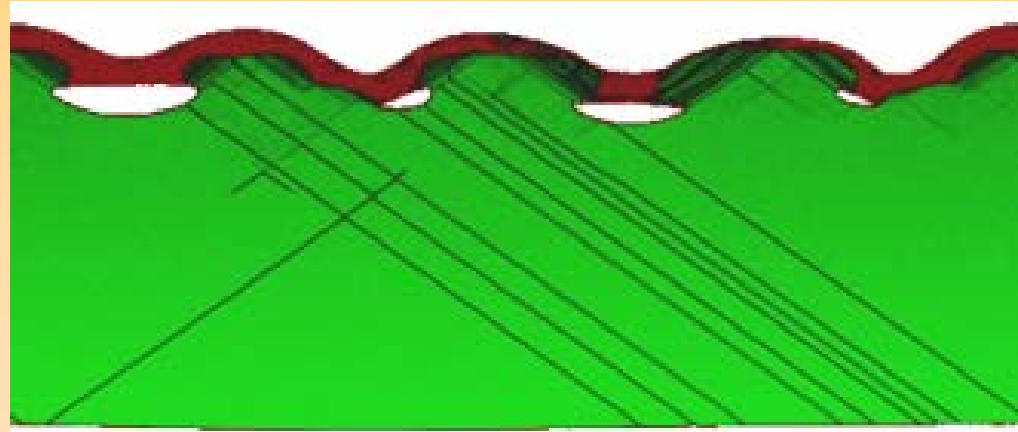
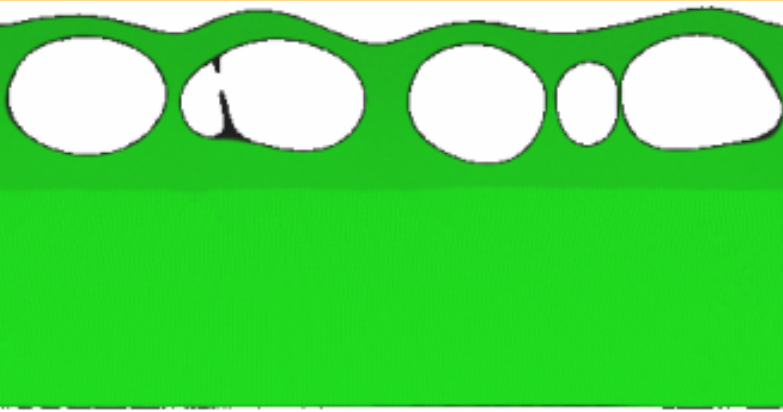
Nucleation in solid state versus nucleation in liquid state

- ❑ To produce foaming and nanostructures melting is necessary. This is the first condition
- ❑ The second condition is: to produce nanostructures we have to be near the ablation threshold, because motion should be slow down significantly to allow to weak surface tension forces to create nanostructures
- ❑ Two-temperature hydrodynamic and molecular-dynamics simulations show that at the ablation threshold LiF nucleates in solid state
- ❑ We can rise fluence and melt LiF but then the second condition will be violated

To find substance with $F_m < F_{abl}$

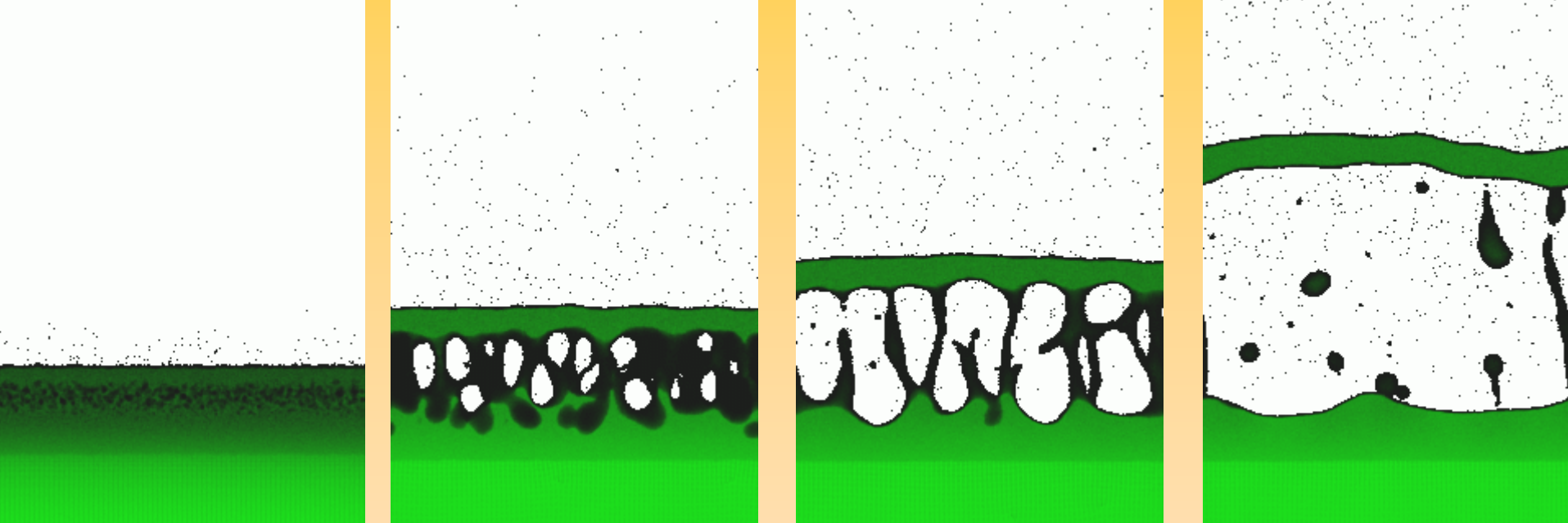
- As was said above to produce surface nanostructures it is necessary to have (condition 2) near threshold spallative ablation in (condition 1) molten material
- Our estimates show that Al is good candidate for this.
- It has small attenuation depth (37 nm, Henke) for our Ag X-ray laser 89.3 eV
- And strong solid state as was shown in our previous simulations. Therefore for Al : the condition (1) $F_m < F_{abl}$ is fulfilled

Examples of nanostructuring by optical lasers



- Our MD simulations and experiment done by Vorobyev and Guo, 2007

**Melting, freezing –
the spallative plate
keeps it connection with target AI**

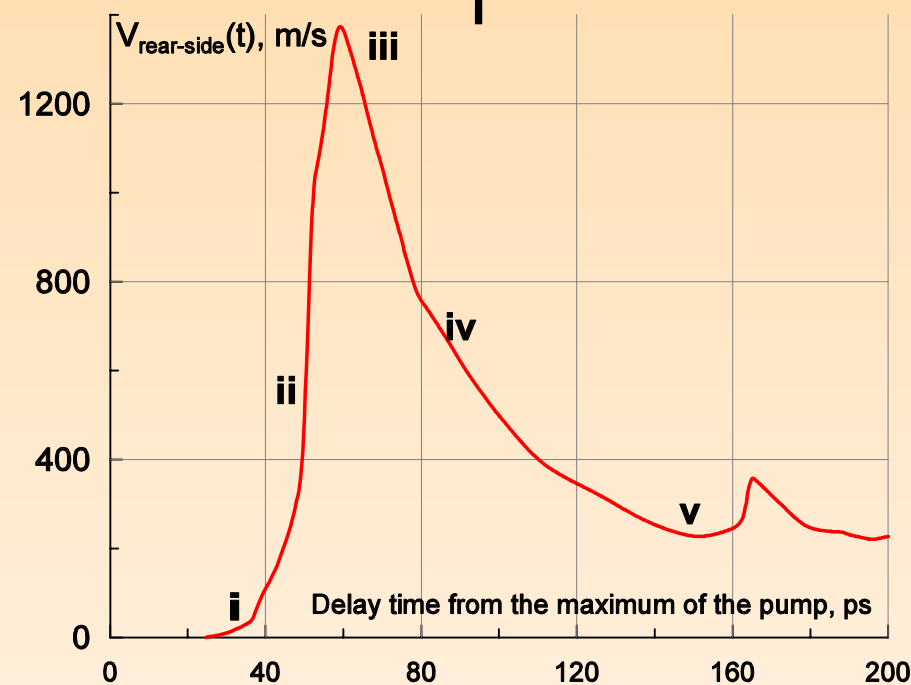
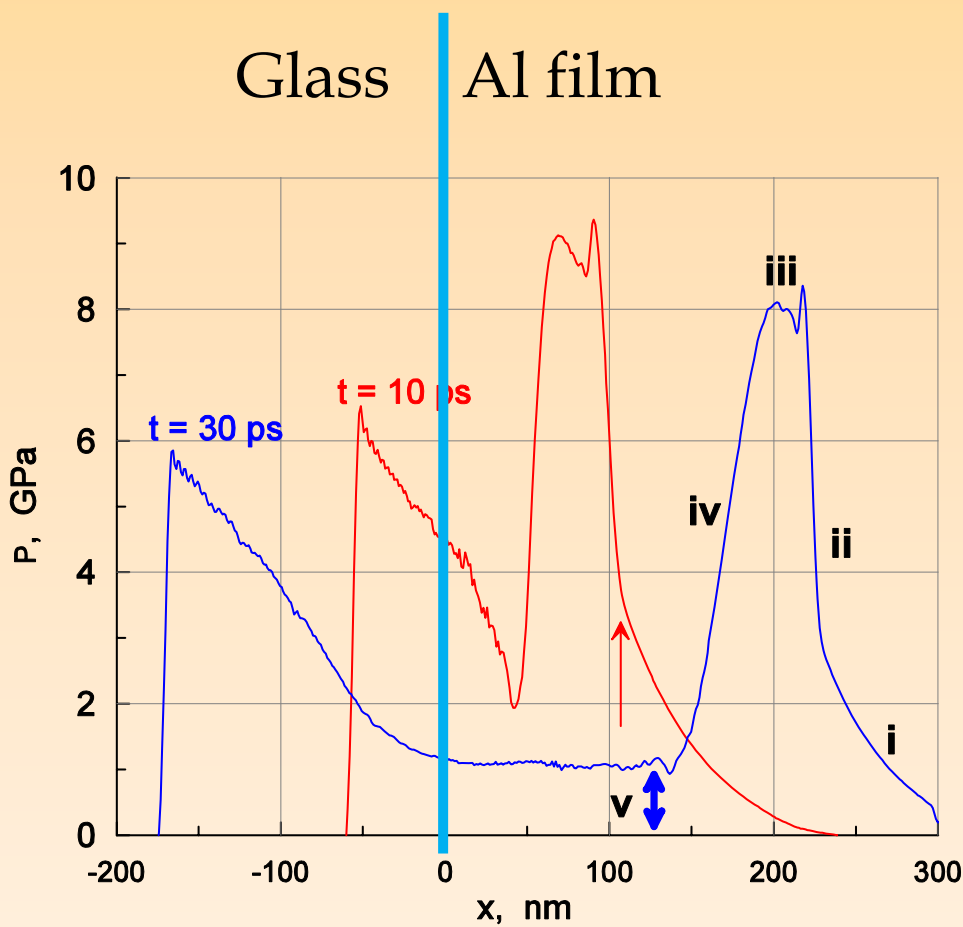
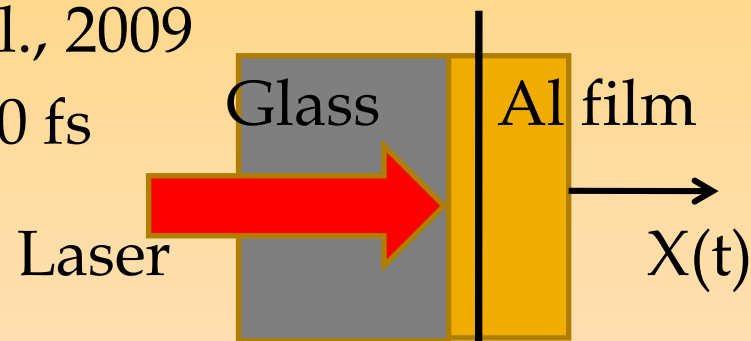


**Nucleation, foaming and nanostructuring
in molten layer of Al.**

**The spallative plate loses
its connection with target**

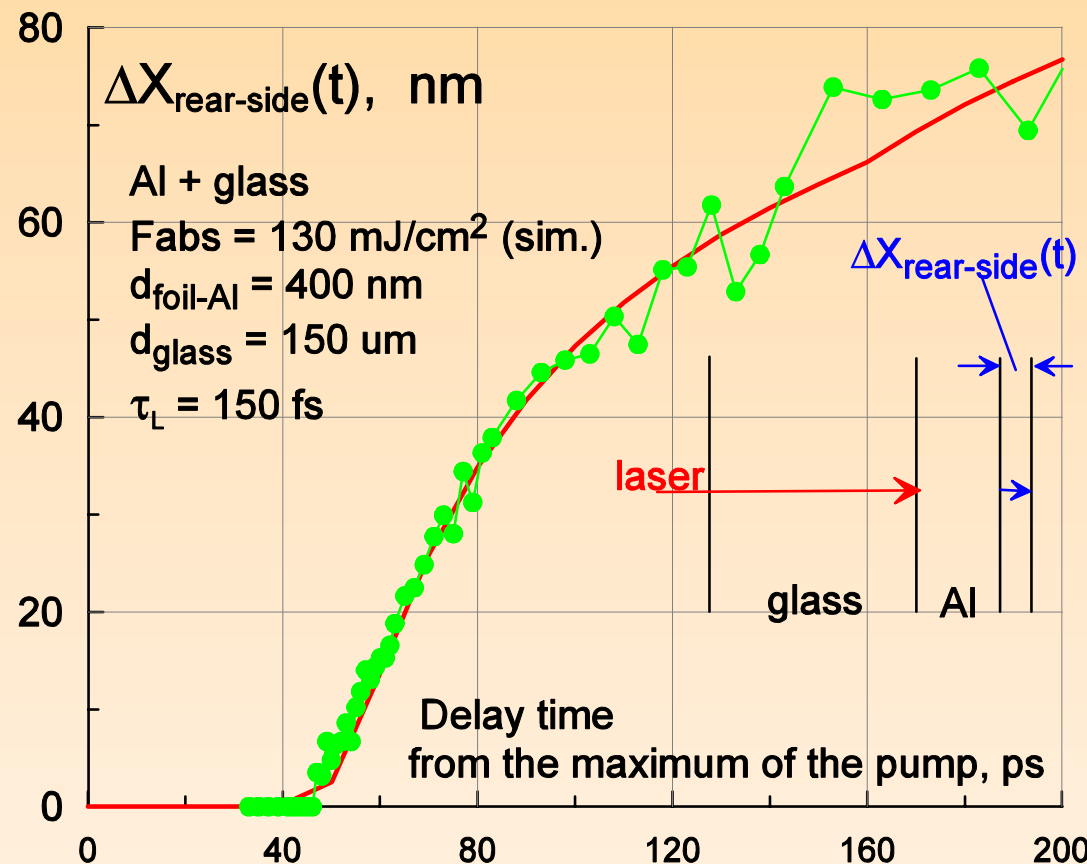
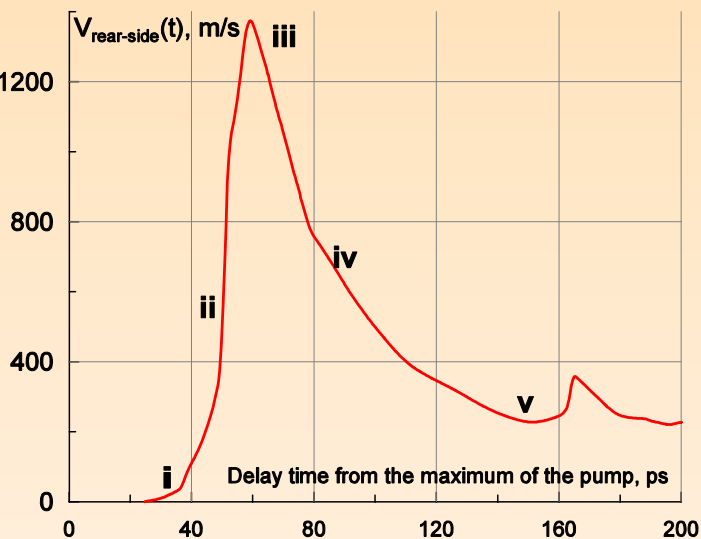
Rear-side spallation and processes in two-temperature layer

- Long pulse lasers, Krasnyuk, Fortov et al., 2002; Eliezer et al., 2002; Krasnyuk, Vovchenko et al., 2009
- Here short pulses, $\tau_L = 40\text{-}200$ fs

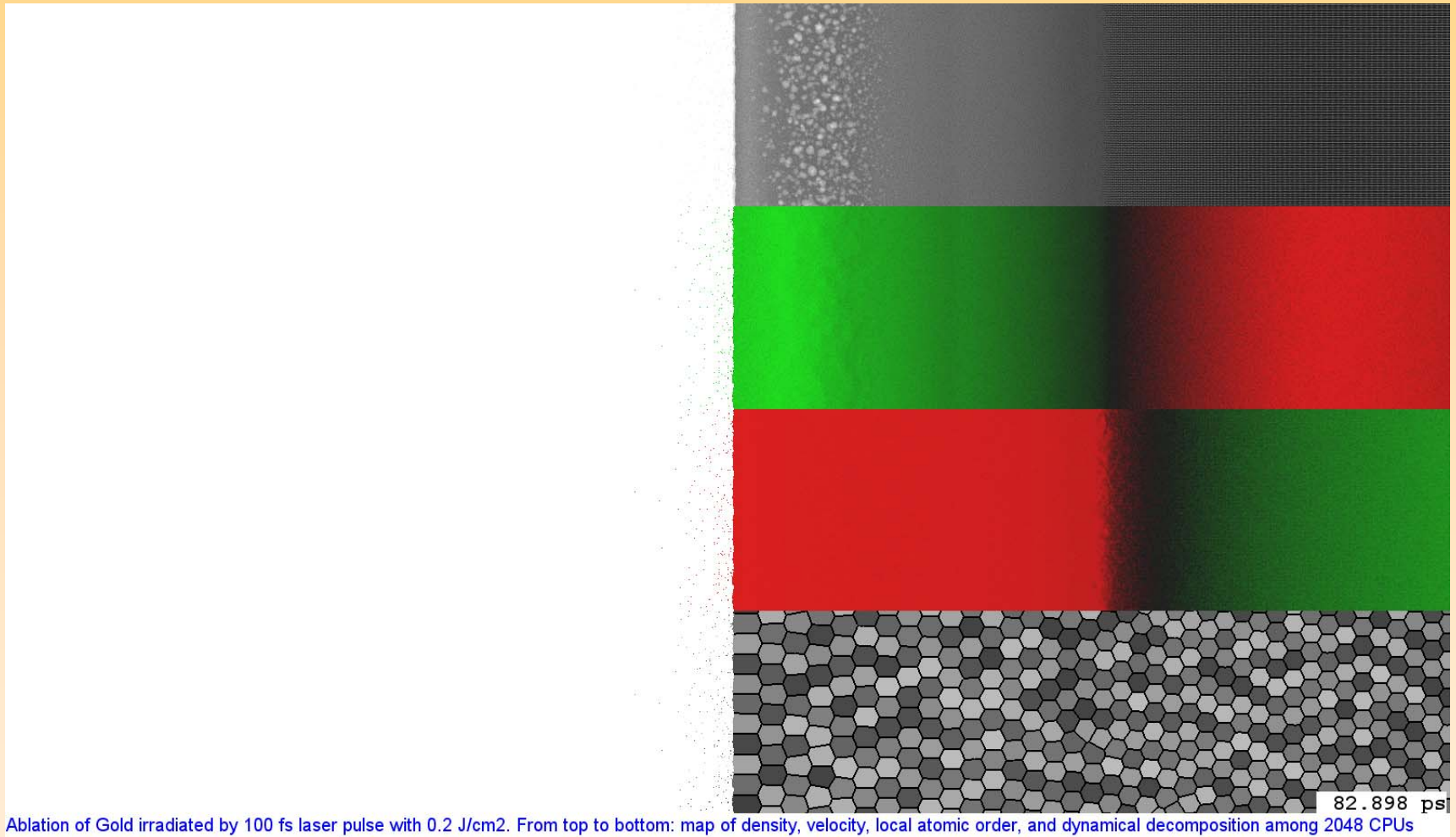


Rear-side spallation and processes in two-temperature layer

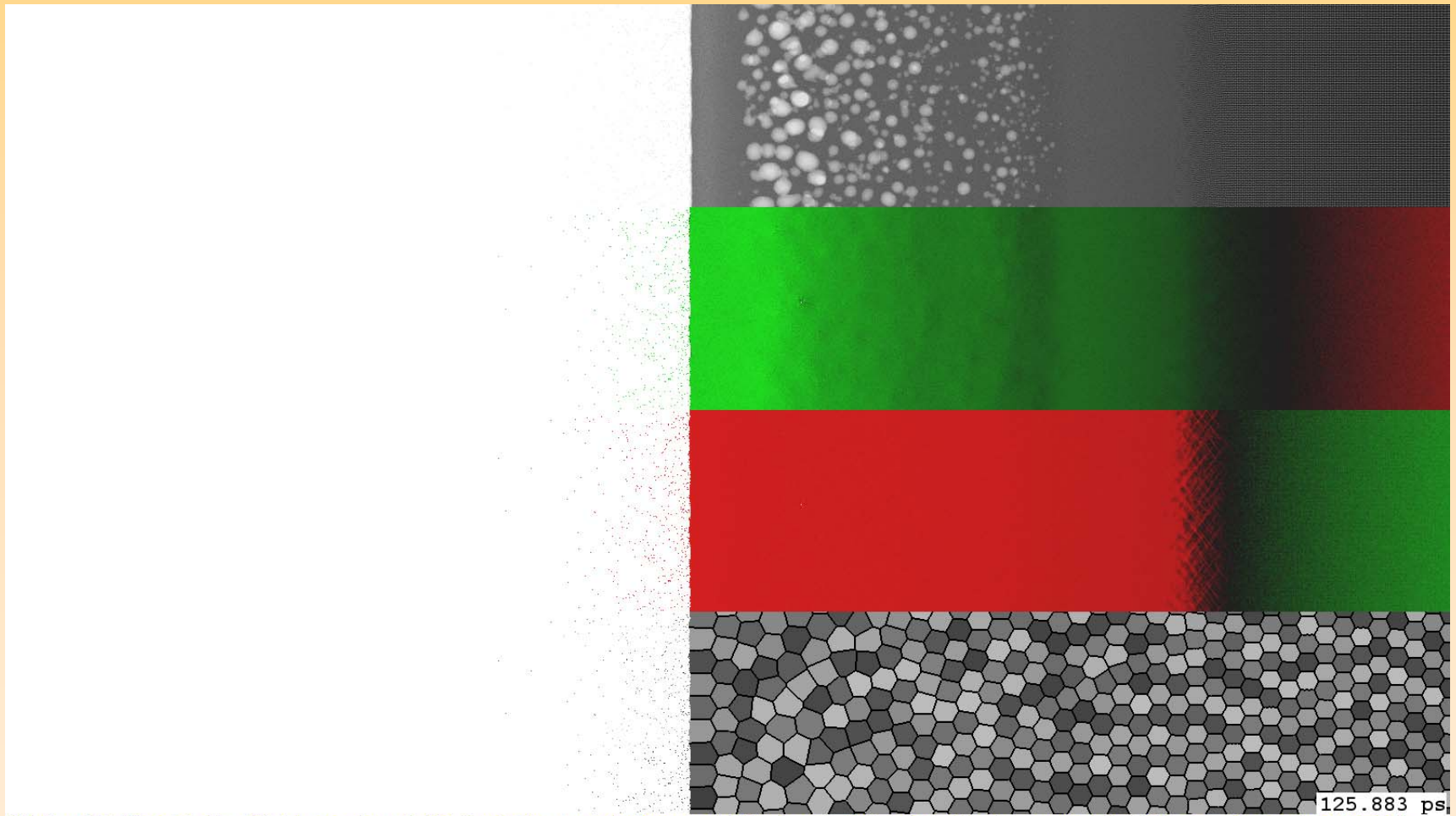
- Non-trivial pressure wave: two-temperature relaxation, fast melting, rarefaction, expansion of molten layer supporting pressure



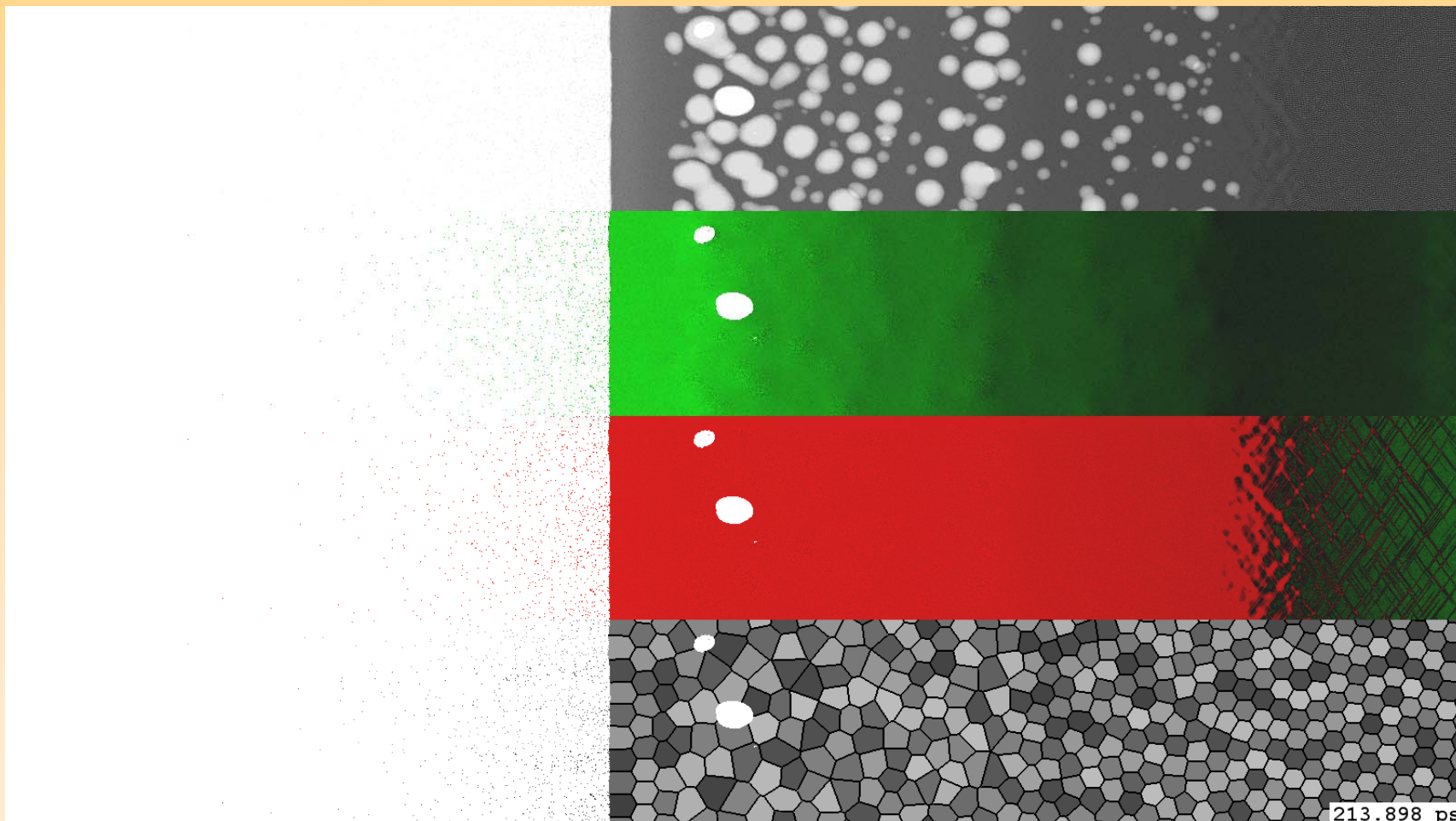
Nucleation and foaming in Au



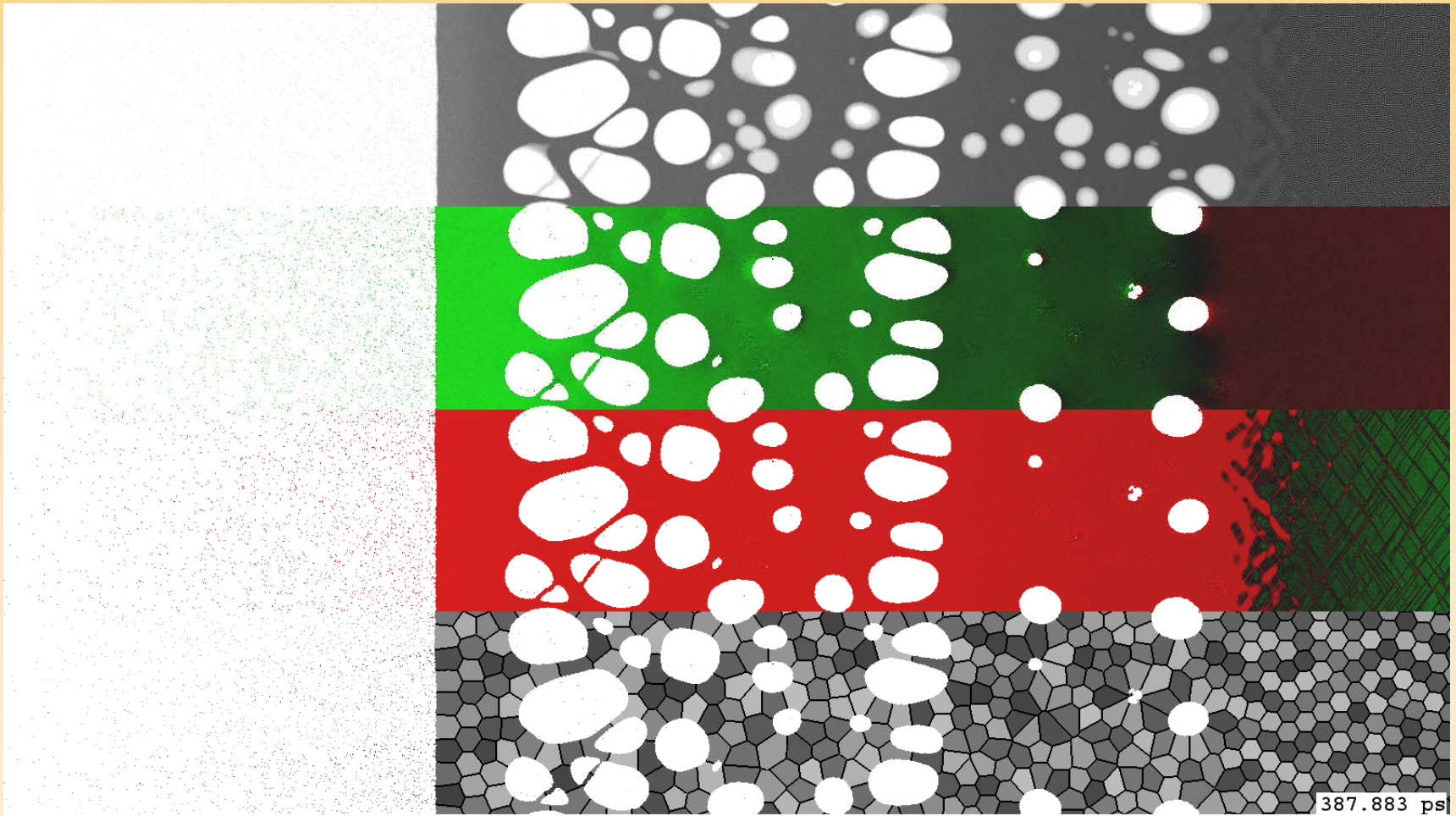
Ablation of Gold irradiated by 100 fs laser pulse with 0.2 J/cm². From top to bottom: map of density, velocity, local atomic order, and dynamical decomposition among 2048 CPUs



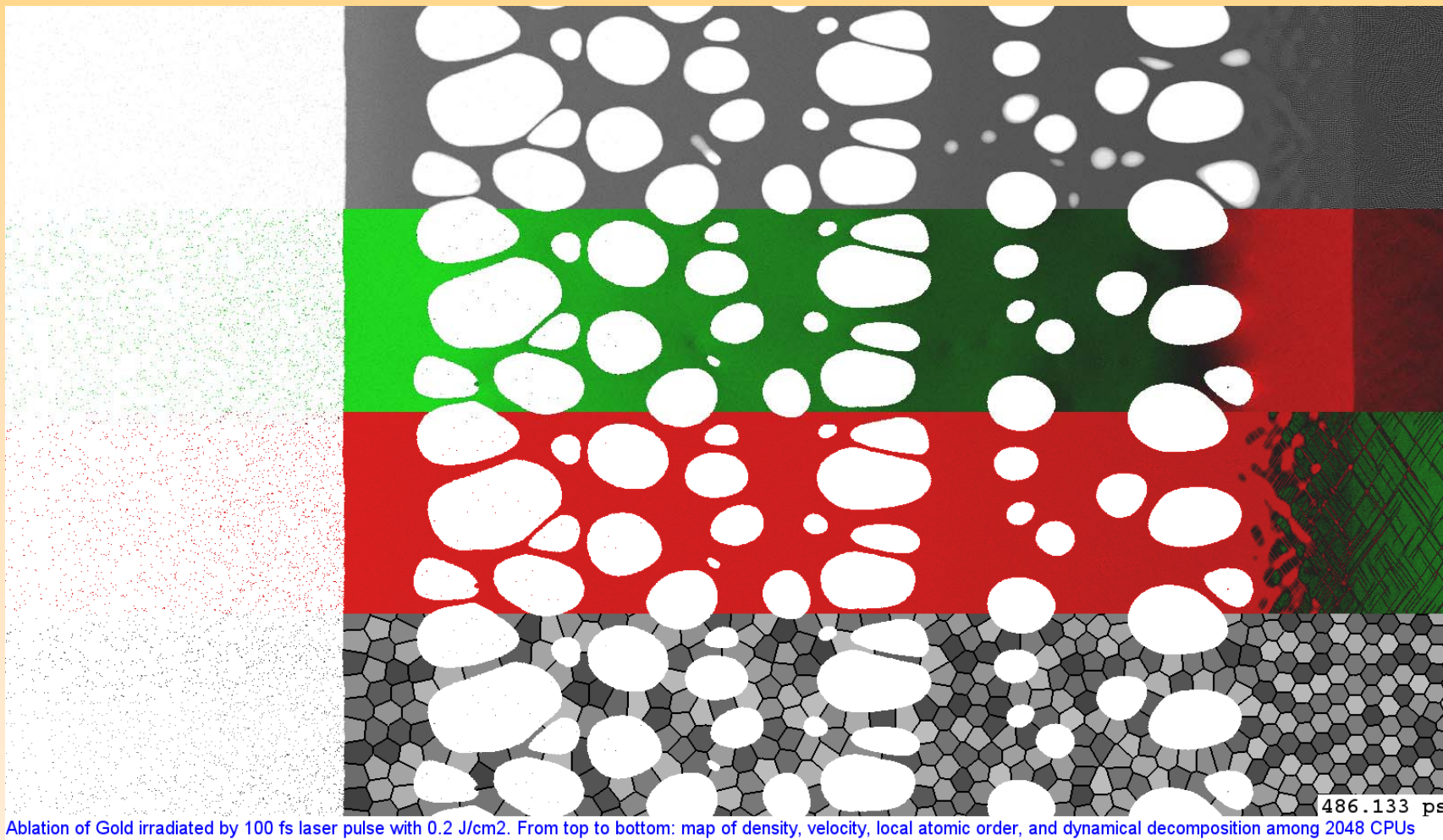
Ablation of Gold irradiated by 100 fs laser pulse with 0.2 J/cm². From top to bottom: map of density, velocity, local atomic order, and dynamical decomposition among 2048 CPUs



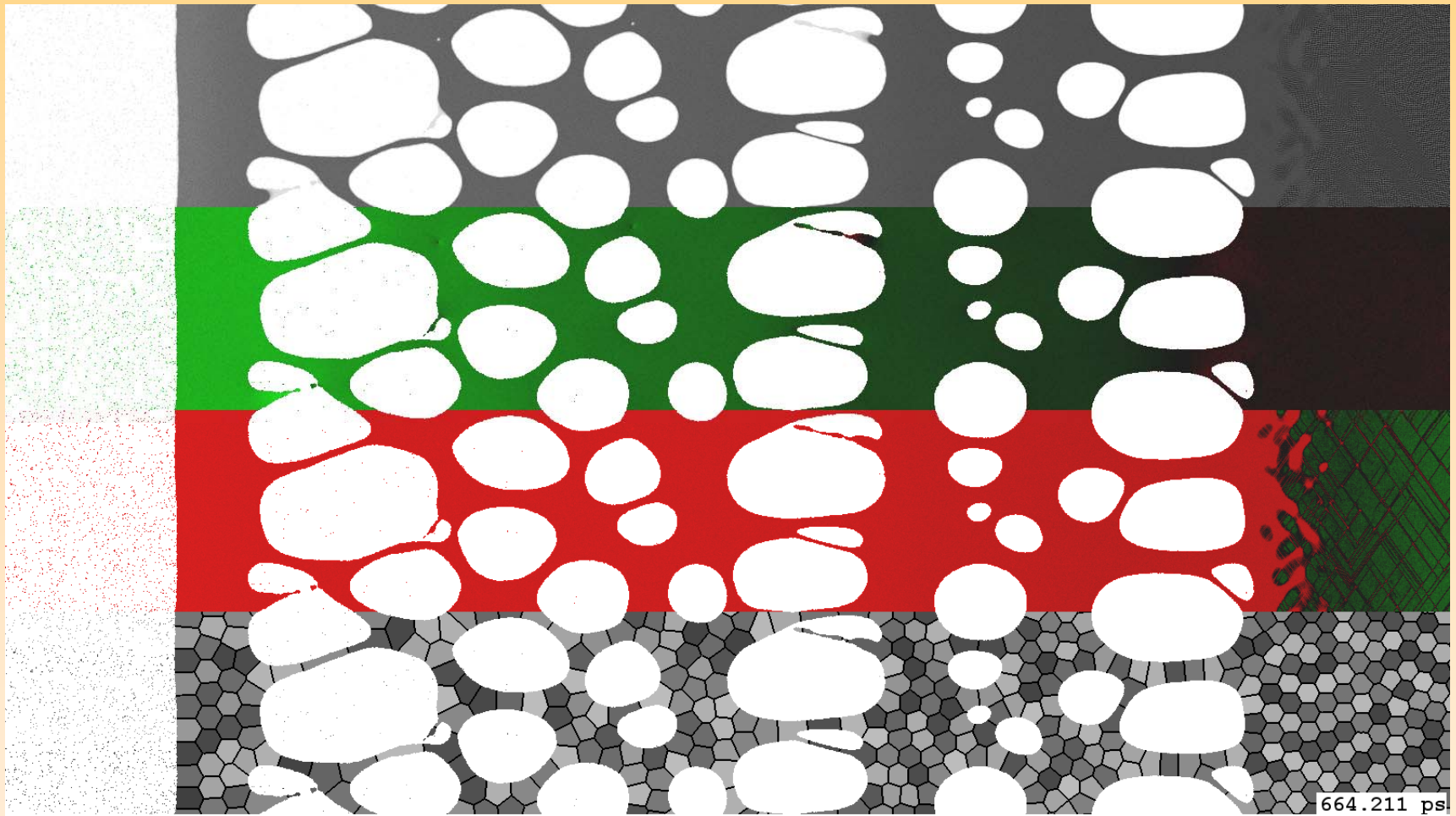
Ablation of Gold irradiated by 100 fs laser pulse with 0.2 J/cm². From top to bottom: map of density, velocity, local atomic order, and dynamical decomposition among 2048 CPUs



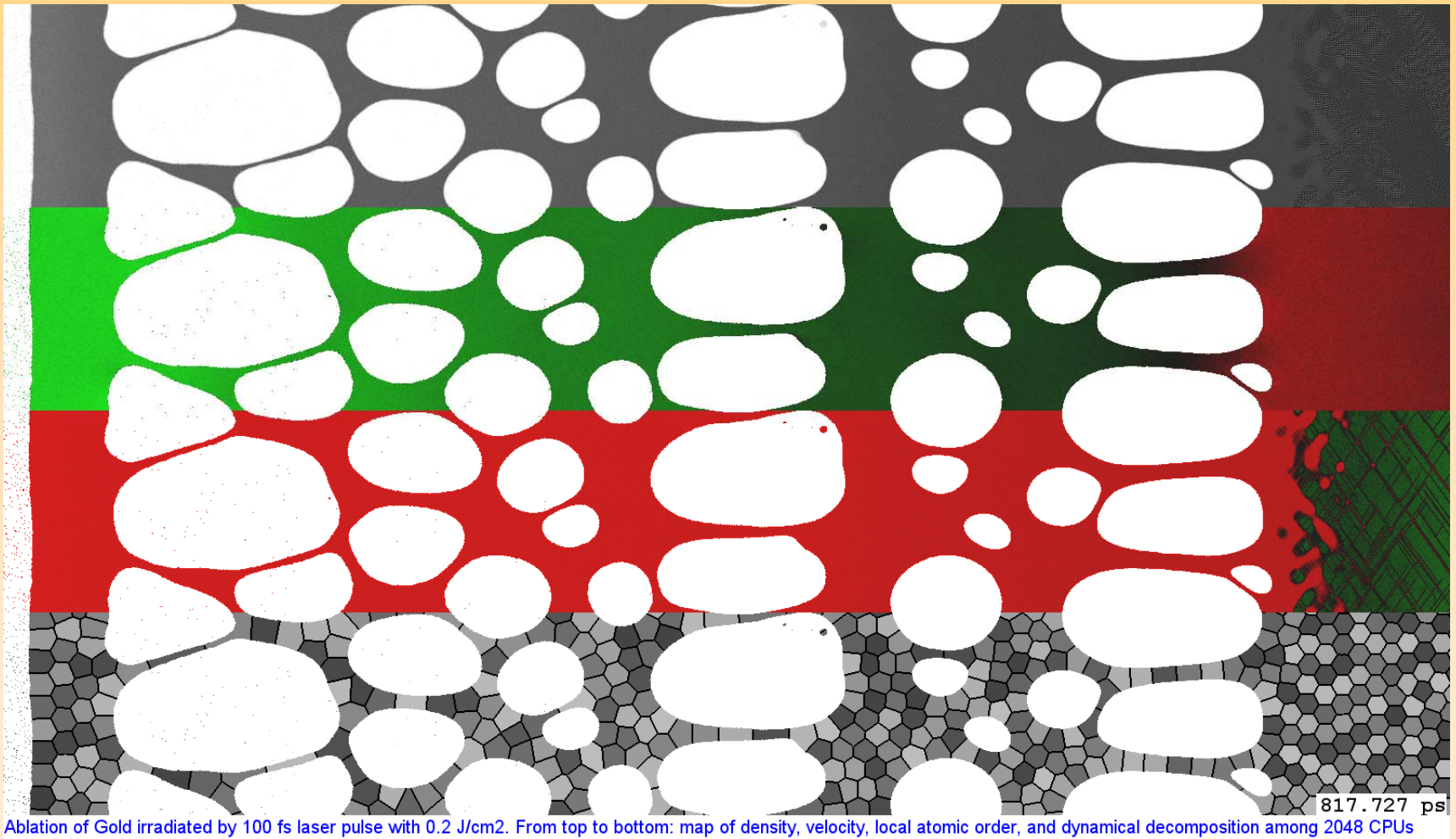
Ablation of Gold irradiated by 100 fs laser pulse with 0.2 J/cm². From top to bottom: map of density, velocity, local atomic order, and dynamical decomposition among 2048 CPUs



Ablation of Gold irradiated by 100 fs laser pulse with 0.2 J/cm². From top to bottom: map of density, velocity, local atomic order, and dynamical decomposition among 2048 CPUs



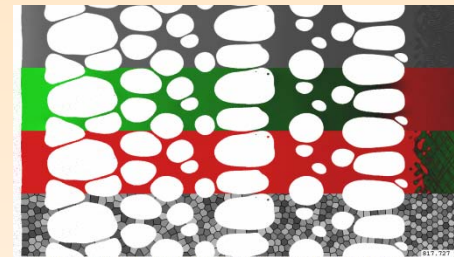
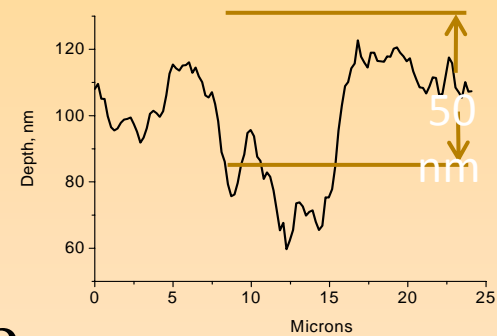
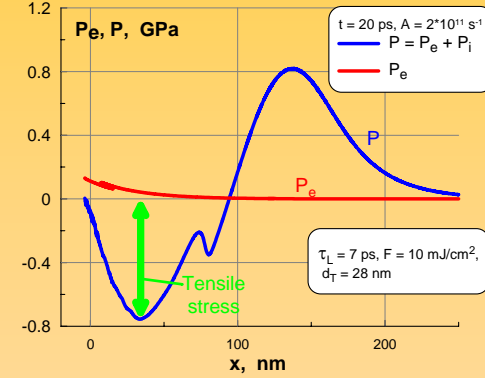
Ablation of Gold irradiated by 100 fs laser pulse with 0.2 J/cm². From top to bottom: map of density, velocity, local atomic order, and dynamical decomposition among 2048 CPUs



Ablation of Gold irradiated by 100 fs laser pulse with 0.2 J/cm². From top to bottom: map of density, velocity, local atomic order, and dynamical decomposition among 2048 CPUs

Conclusion

- Short X-ray pulse produces tensile stress (theory)
- Experiments show that X-ray ablation with low threshold exists
- Then X-ray laser may produce spallative ablation as it is now well known for optical short pulse lasers
- Near ablation threshold this may (if the X-ray $F_m < F_{abl}$) cause nanostructuring

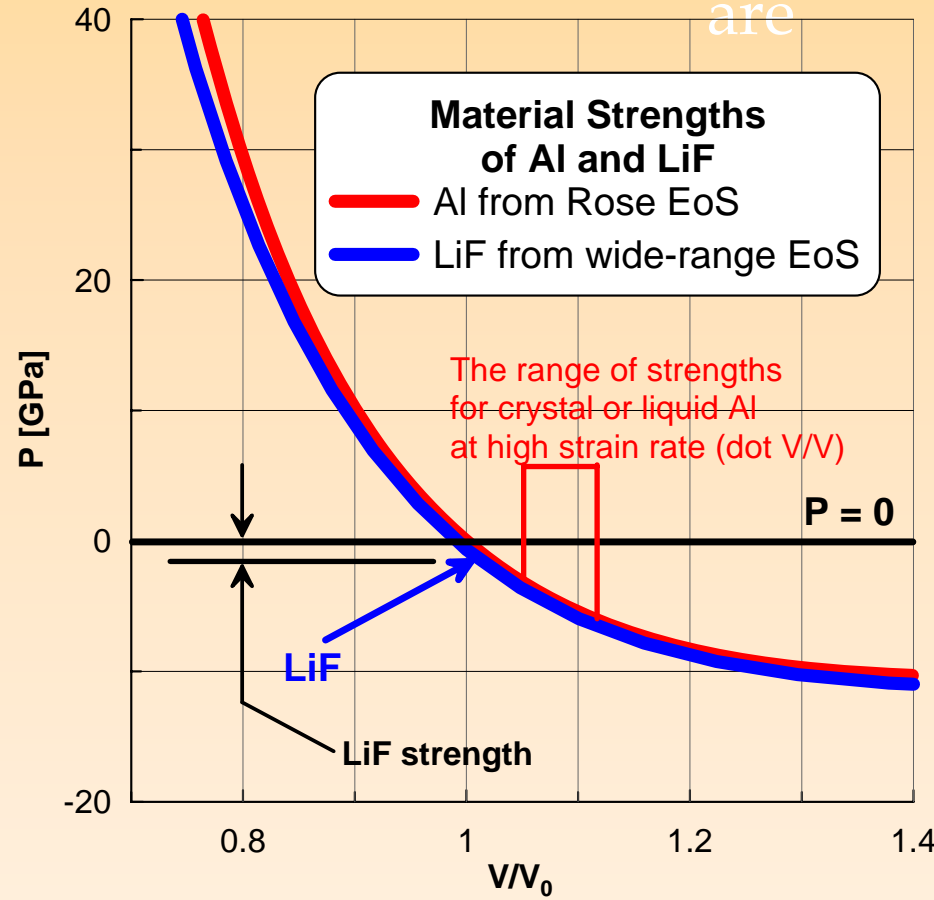


Equation of state (EoS)

- EoS is necessary to simulate energy absorption (heating) together with dynamics
- We compare EoS for LiF and Al from the cite ..\rusbank created by Khishchenko, Lomonosov, Levashov, Fortov, et al.
- In our form of presentation equations only P_{at} and E_{at} are used

- $P_{at} = G * E_{at}$ and $P_{at}(\rho, T=0)$ are similar for LiF and Al (G=Grueneisen parameter)

- Therefore we use EOS fo Al to simulate LiF
- The only open question concerns the material strength for LiF
- LiF is brittle material -its strength should be small in comparison with metals

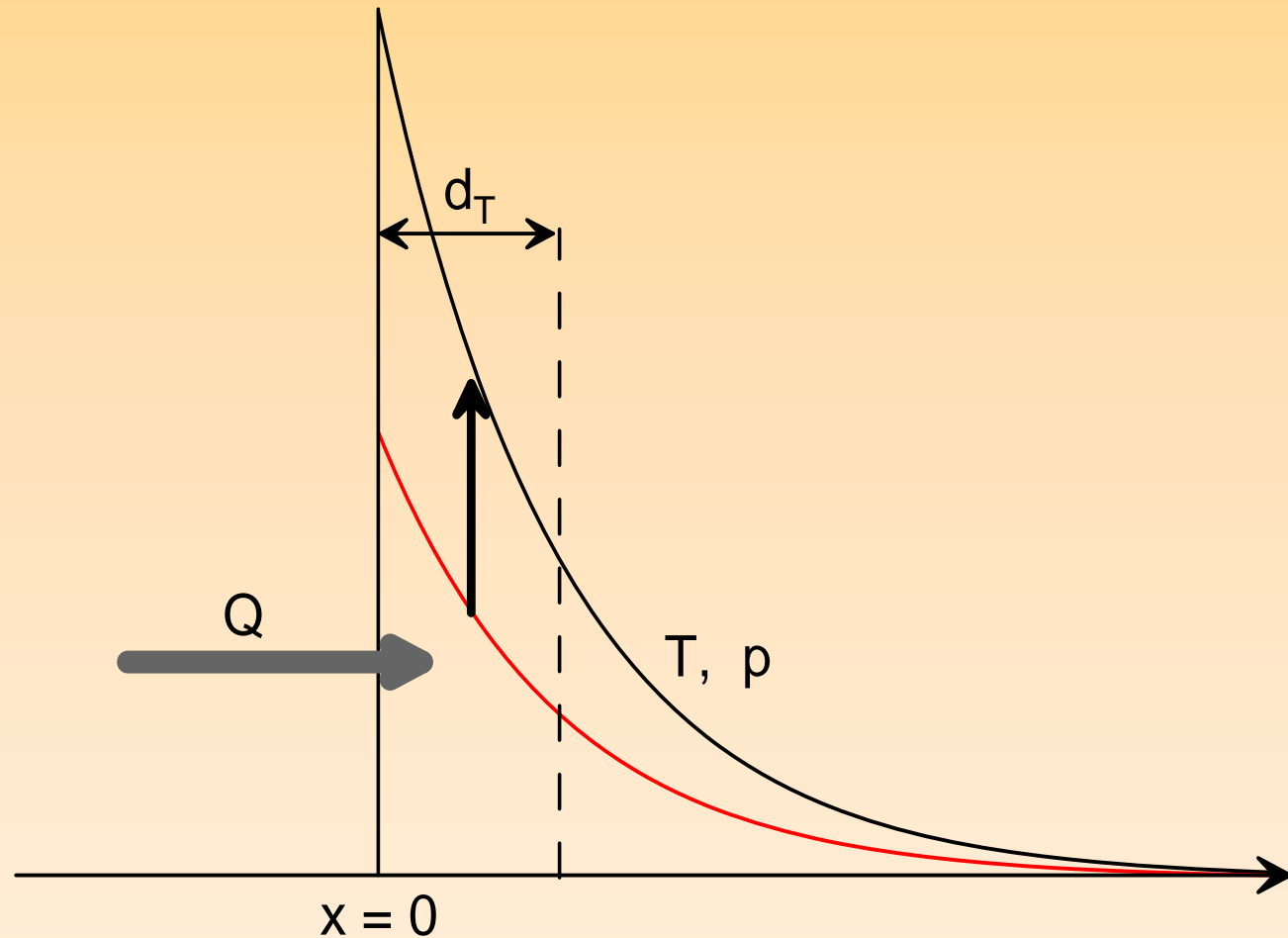


Spallative mechanism: how it works

- ▣ **(1)** Temperature rise – it should be fast! How fast? Faster than sonic relaxation
- ▣ **(2)** Pressure rise
- ▣ **(3)** Acoustic relaxation: decomposition into waves → wave reflection from vacuum boundary of a plane target → reflection creates negative pressures (tensile stress)
- ▣ **(4)** Strength of material: ability to resist to stretching and tensile stress. Limiting strength. Sharp ablation threshold

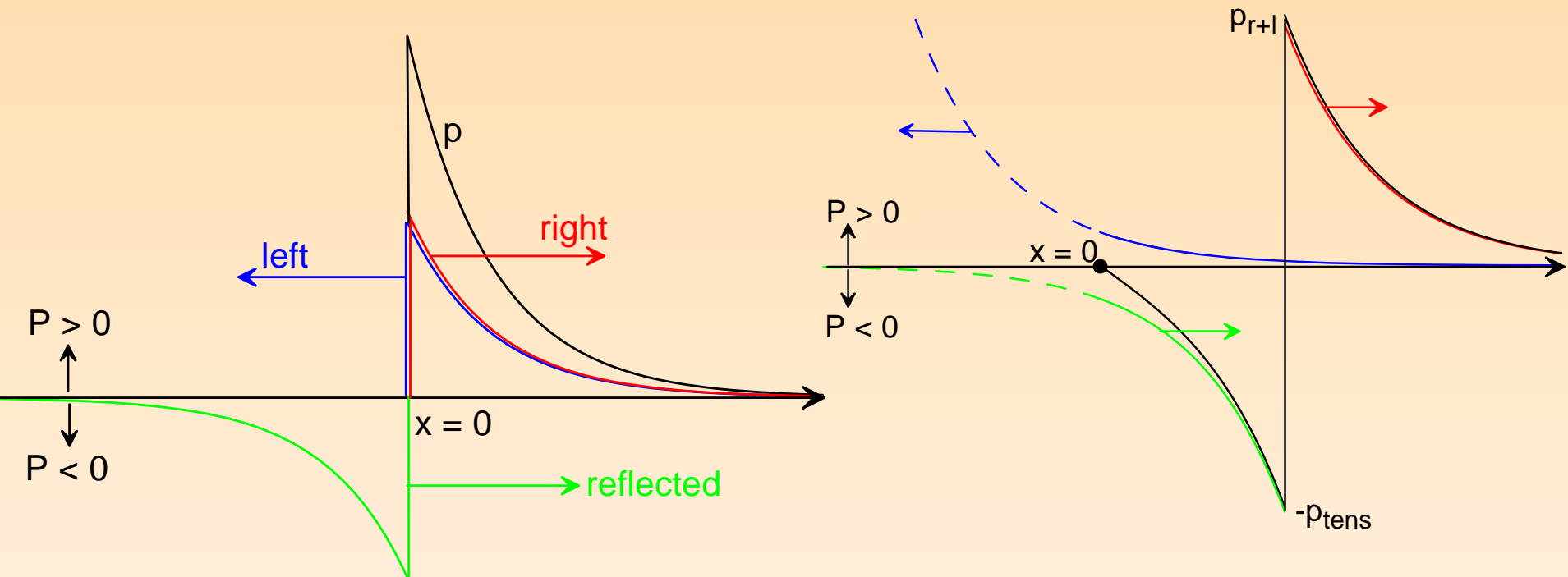
(1), (2) Fast temperature rise.
If it is fast then P also increases

- ▣ Thickness of the layer heated by laser is d_T
- ▣ Sonic relaxation time is $t_s = d_T / c_s$
- ▣ Fast means that duration of laser pulse τ_L is smaller than t_s



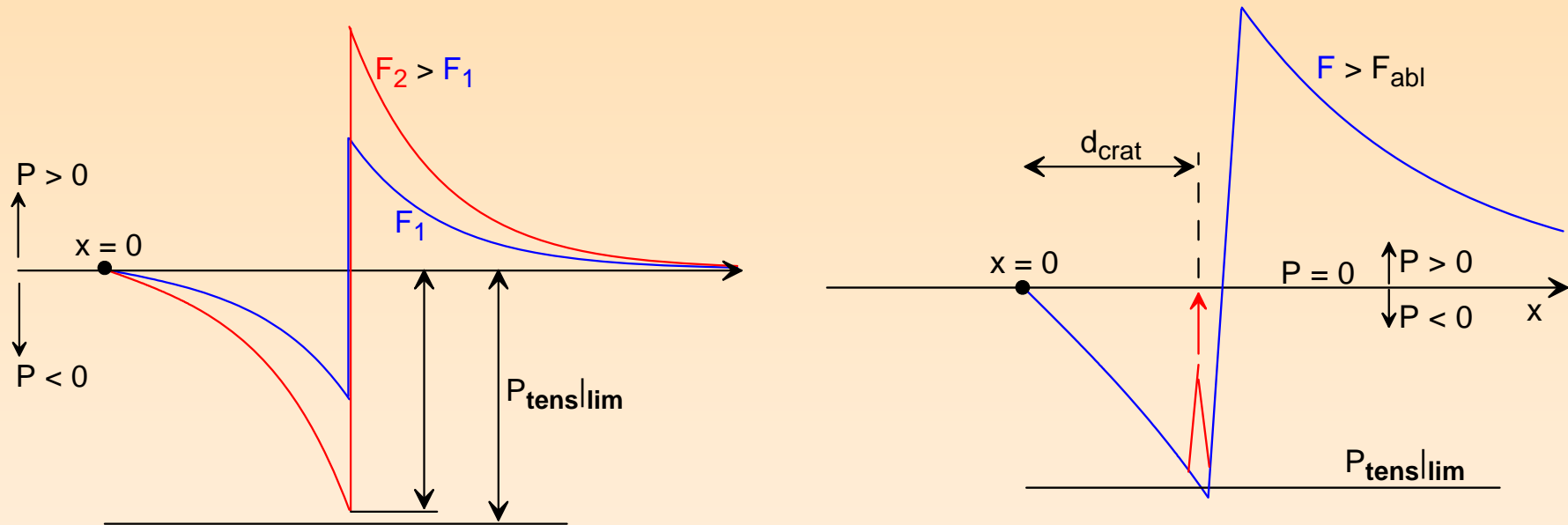
(3) D'Alembert waves

- Acoustic decomposition: solutions of the wave equation $d_{tt}P - c^2 d_{xx}P = 0$: $P = P_+(x+ct) + P_-(x-ct)$
- Reflection from boundary with vacuum: therefore there are three waves: left, right, and reflected



(4) Limiting strength of material

- ▣ $P_{\text{tensile}} \mid \text{limiting}$. This is why there is a sharp threshold F_{abl} for spallative ablation
- ▣ Rupture takes place at a finite depth under vacuum boundary, therefore a finite piece of removed (=ablated) material appears



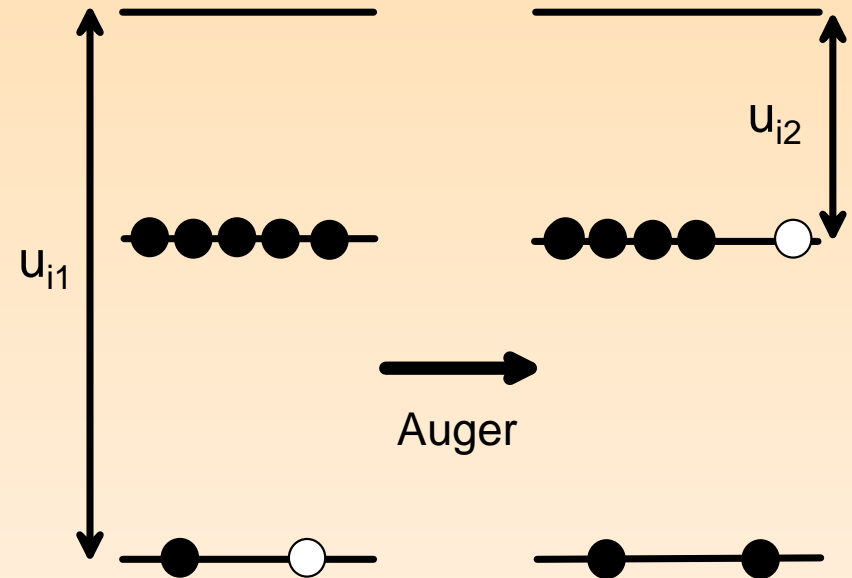
(IR-visible) laser \rightarrow metals or dielectrics

- ▣ Introduction of spallative ablation (Inogamov et al., 1999) solves the puzzle of Newton rings observed in pump-probe experiments at all metals and semiconductors (universality of this phenomenon), Sokolowski-Tintev, von der Linde, et al., 1998
- ▣ Owing to this mechanism combination of two-temperature physics together with thermodynamic properties of condensed material becomes important
- ▣ The mechanism explains existence of sharp ablation threshold
- ▣ The laser plume has unusual shape with flying cupola around liquid-vapor mixture. Cupola remains in condensed state. Therefore density profile in the plume is non-monotonous
- ▣ Near threshold irradiation forms nanorelief at surface

X-rays \rightarrow dielectrics

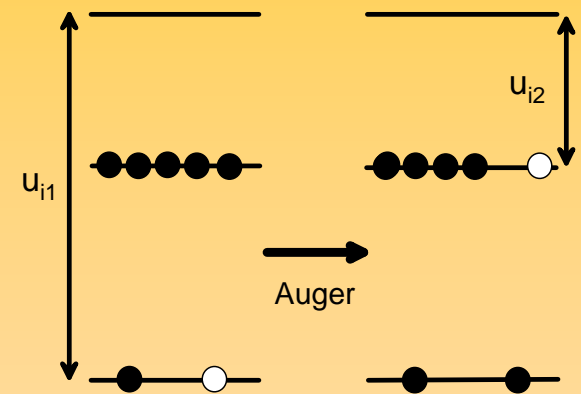
- ▣ Our case is: 90 eV photons, $\tau_L = 7$ ps, Fluence = 5 – 10 mJ/cm²
- ▣ Absorption, attenuation length in LiF is 28 nm
- ▣ Photoionization, primary ions are single charged (Z=1) Li 1s2s, F 1s² 2s 2p⁵. Z mainly =1 because ion concentration is low ($\sim 1\%$)

- Auger recombination from primary ions to Z=1 ions with a hole at external electronic shell



Kinetics of secondary ions u_{i2}

- Ions gradually disappear as result of cooling of initially hot electron subsystem due to energy transfer to cold



$$dn_e/dt = Q/u_{i2} + \nu_{imp}n_e - \kappa_{rec}n_e^3, \quad Q = (F/(\sqrt{\pi}d_T\tau_L)) \exp(-t^2/\tau_L^2),$$

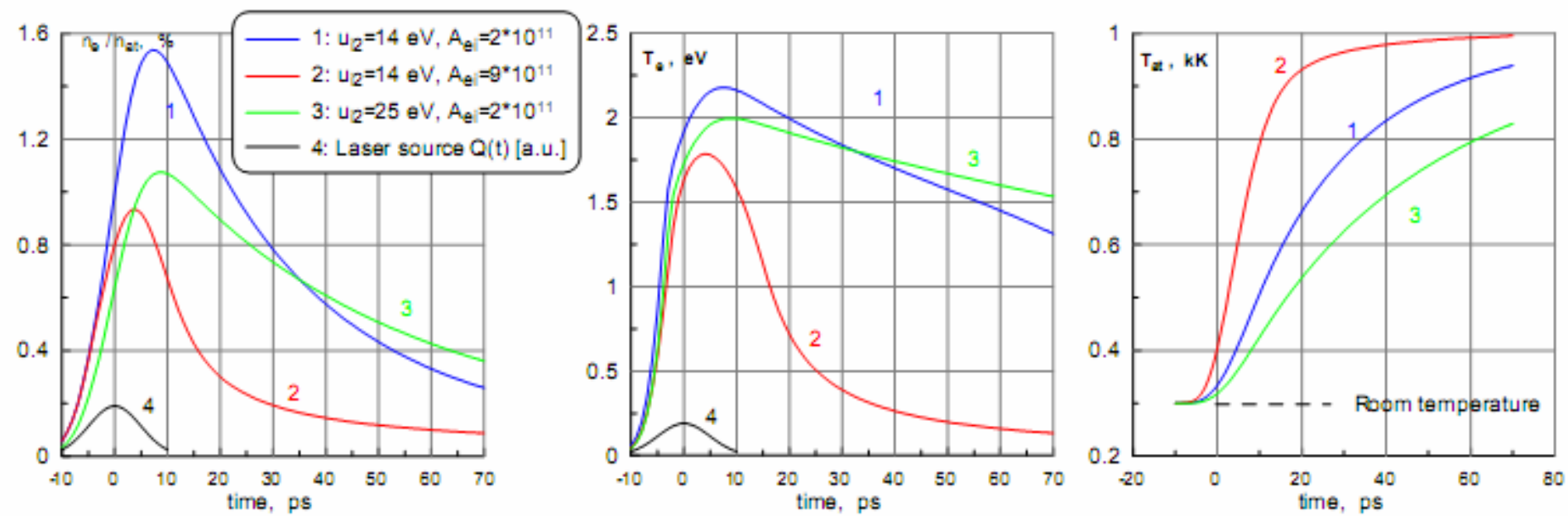
$$dE_e^s/dt = Q - \dot{E}_{ea}, \quad E_e^s = n_e u_{i2} + E_e, \quad E_e = (3/2)n_e T_e,$$

$$CdT_{at}/dt = \dot{E}_{ea}, \quad C \approx 6k_B n_c, \quad n_c \approx 6 \cdot 10^{22} \text{ cm}^{-3}, \quad \dot{E}_{ea} = AE_e,$$

- Q/u_{i2} is a X-ray source of free electrons, $\nu_{imp} = \langle v \cdot \sigma \rangle n_{at}$ is a frequency of ionization by an electron impact, κ_{rec} is a coefficient of three body recombination
- E_e^s is total energy of electron subsystem, it is a sum of potential and thermal energies
- \dot{E}_{ea} is an energy exchange rate between atomic and electron subsystems. This is the only term taking away energy of electron subsystem – radiation losses are small at our time scale

Energy transfer from X-ray photons to atoms through electronic subsystem

- Increase and decrease of free electron population: influence of ionic potential u_{i2} is rather small, while influence of the coefficient A in $\dot{E}_{ea} = A \cdot E_e$ is rather significant. The rate \dot{E}_{ea} is connected with almost elastic collisions of the conductivity band electrons with atoms
- This is solution of ODE for $\{n_e, T_e\}$ neglecting acoustic effects



Combination of kinetic, thermal, and sonic effects

$$\rho^\circ \frac{\partial}{\partial t} \frac{E_e}{\rho} = \frac{\rho^\circ}{\rho} Q - \frac{\rho^\circ}{\rho} \dot{E}_{\epsilon a} - p_e \frac{\partial u}{\partial x^\circ} + \frac{\partial}{\partial x^\circ} \left(\frac{\rho \kappa_e}{\rho^\circ} \frac{\partial T_e}{\partial x^\circ} \right)$$

$$\rho^\circ \partial u / \partial t = -\partial p / \partial x^\circ$$

$$\rho^\circ \partial (E_{at} / \rho) / \partial t = (\rho^\circ / \rho) \dot{E}_{\epsilon a} - p_{at} \partial u / \partial x^\circ + (\partial / \partial x^\circ) ((\rho \kappa_{at} / \rho^\circ) \partial T_{at} / \partial x^\circ)$$

- System of hydrodynamic equations: two thermal eqs. for E_e and E_{at} and eq. for momentum
- We neglect here equation for n_e
- Corresponding space homogeneous eq. is $\dot{E}_e = Q - A E_e$
- We call this eq. {Ee}
- It has main terms: X-ray heating Q and $e \rightarrow a$ cooling

Comparison of $\{n_e, T_e\}$ and $\{E_e\}$ eqs

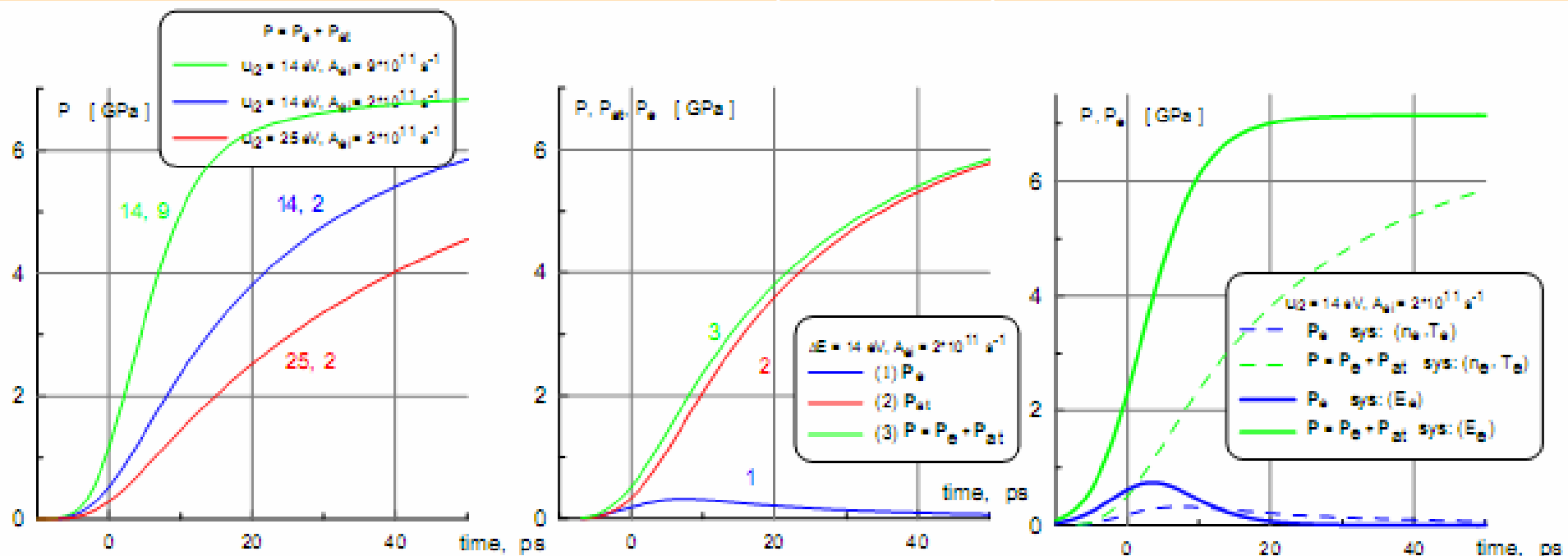
$$dn_e/dt = Q/u_{i2} + \nu_{imp}n_e - \kappa_{rec}n_e^3, \quad Q = (F/(\sqrt{\pi}d_T\tau_L)) \exp(-t^2/\tau_L^2),$$

$$dE_e^s/dt = Q - \dot{E}_{ea}, \quad E_e^s = n_e u_{i2} + E_e, \quad E_e = (3/2)n_e T_e,$$

$$CdT_{at}/dt = \dot{E}_{ea}, \quad C \approx 6k_B n_c, \quad n_c \approx 6 \cdot 10^{22} \text{ cm}^{-3}, \quad \dot{E}_{ea} = AE_e,$$

$$\dot{E}_e = Q - AE_e$$

The worst case with small A and therefore slow e-a energy transfer is shown. Conclusion from this comparison is: the $\{E_e\}$ approach may be used for estimates of pressure amplitudes



Experimental results

- ▣ Measured ablation threshold is surprisingly low! **Only 10 mJ/cm²**. To understand that this is indeed unexpected it is enough to compare this threshold with typical thresholds of several thousands mJ/cm² for dielectrics for IR-vis. lasers (fs-ns duration) and with 100 mJ/cm² threshold for X-ray 1.7 ns laser → duration is important (our XRL has $\tau_L = 7$ ps)
- ▣ The crater depth is approximately 50 nm

Conclusion

- ▣ Experimentally very low ablation threshold has been found
- ▣ Theory explains this as transition from evaporative to spallative ablation